Graduate School Form 30
Updated 1/15/2015

PURDUE UNIVERSITY
GRADUATE SCHOOL
Thesis/Dissertation Acceptance

This is to certify that the thesis/dissertation prepared

By Tanja L. Greene

Entitled

MODULAR CROSSLINKING OF GELATIN BASED THIOL-NORBORNENE HYDROGELS FOR IN VITRO 3D CULTURE OF HEPATIC CELLS

For the degree of Master of Science in Biomedical Engineering

Is approved by the final examining committee:

Chien-Chi Lin
Chair

Dong Xie

Guoli Dai

To the best of my knowledge and as understood by the student in the Thesis/Dissertation Agreement, Publication Delay, and Certification Disclaimer (Graduate School Form 32), this thesis/dissertation adheres to the provisions of Purdue University's "Policy of Integrity in Research" and the use of copyright material.

Approved by Major Professor(s): Chien-Chi Lin

Approved by: Ken Yoshida 12/3/2015

Head of the Departmental Graduate Program Date

MODULAR CROSSLINKING OF GELATIN BASED THIOL-NORBORNENE HYDROGELS FOR *IN VITRO* 3D CULTURE OF HEPATIC CELLS

A Thesis

Submitted to the Faculty

of

Purdue University

by

Tanja L. Greene

In Partial Fulfillment of the

Requirements for the Degree

of

Master of Science in Biomedical Engineering

December 2015

Purdue University

Indianapolis, Indiana

ACKNOWLEDGMENTS

First and foremost, I would like to extend my everlasting appreciation to my thesis advisor, Dr. Chien-Chi Lin. He provided me an opportunity to learn and develop throughout the entirety of this research and thesis work. Through support, encouragement, and most of all direction, Dr. Lin compassionately shared with me previous research skills and allowed me to gain beneficial knowledge and experience for which I will continually be grateful.

Second, I would like to thank my advisory committee members, Dr. Dong Xie and Dr. Guoli Dai, for their time and input during the completion of this thesis work.

In addition, I would like to thank my colleagues: Dr. Tsai-Yu Lin and Ms. Han Shih for their discussion and input, Mr. John Bragg, Mr. Brent Hukill, and Mr. Camron Dawes for their support. I would also like to thank undergraduate alumni Zach Munoz for his characterization of GelNB synthesis, Sherry Clemens for her assistance with documentation, and Mrs. Valerie Lim Diemer for her guidance in thesis formatting.

Finally, a huge thank you is due to my family and friends for their continued support and belief in my betterment and educational career. Without their understanding and willingness to help me outside of academics, as I am a non-traditional student, my focus would not have been able to be solely on my education. For this I am endlessly indebted.

TABLE OF CONTENTS

Page

LIST OF TABLES

LIST OF FIGURES

Figure Page

Figure Page

Appendix Figure

SYMBOLS

G’	elastic (storage) modulus, (Pa)
Hz	hertz
M	molar
N	normal
R	ratio of thiol moieties to ene moieties
W_o	the intital mass of hydrogel, (mg)
W_t	hydrogel weight measured at specified time points, (mg)

ABBREVIATIONS

2D	two dimensional
3D	three dimensional
ANOVA	analysis of variance
Arg	arginine (amino acid)
Asp	aspartic acid (amino acid)
BSA	bovine serum albumin
CYP450/3A4	cytochrome P450/3A4
ddH_2O	double distilled water
DMEM	Dulbecco's modified eagle medium
DMMB	1,9-Dimethyl-methylene Blue
DMSO	Dimethyl sulfoxide
DPBS	Dulbecco's phosphate buffered saline
ECM	Extracellular matrix
EDC	1-Ethyl-3-(3-dimethylaminopropyl) carbodiimide
ELISA	Enzyme linked immunosorbent assay
FBS	Fetal bovine serum
GAG	Glycosaminoglycan
GelMA	Gelatin-methacrylate
GelNB	Gelatin-norbornene
GelNB-A	Type A gelatin-norbornene
GelNB-A-Hep	Type A gelatin-norbornene heparin conjugated
GelNB-B	Type B gelatin-norbornene
GelNB-B-Hep	Type B gelatin-norbornene heparin conjugated
Gly	Glycine (amino acid)

HGF	Hepatocyte growth factor
HepaRG	Human hepatic progenitor cells
HNF4α	Hepatocyte nuclear factor 4 alpha (hepatocyte specific gene)
Huh7	Human-derived hepatocellular carcinoma cells
HUVEC	Human umbilical vein endothelial cells
LAP	Lithium acylphosphinate
MMP	Matrix metalloproteinases
MWCO	Molecular weight cutoff
NHS	N-Hydroxysuccinimide
NTCP	Na^+/Taurocholate co-transporting polypeptide (hepatocyte specific gene)
PBS	Phosphate buffered saline
PEG	Poly(ethylene glycol)
PEGDA	Poly(ethylene glycol)-diacrylate
PEG4NB	Poly(ethylene glycol)-tetra-norbornene
PEGOH	Poly(ethylene glycol)-hydroxyl
PEG4SH	Poly(ethylene glycol)-tetra-thiol
PEGSH	Poly(ethylene glycol)-thiol
pI	Isoelectric point
rhBMP-2	Recombinant human bone morphogenic protein 2
TCP	Tissue culture plastics
UV	Ultraviolet
Vol	Volume
W or Wt	Weight

ABSTRACT

Greene, Tanja L. M.S.B.M.E., Purdue University, December 2015. Modular Crosslinking of Gelatin Based Thiol-Norbornene Hydrogels for *In Vitro* 3D Culture of Hepatic Cells. Major Professor: Chien-Chi Lin.

As liver disease becomes more prevalent, the development of an *in vitro* culture system to study disease progression and its repair mechanisms is essential. Typically, 2D cultures are used to investigate liver cell (e.g., hepatocyte) function *in vitro*; however, hepatocytes lose function rapidly when they were isolated from liver. This has promoted researchers to develop 3D scaffolds to recreate the natural microenvironment of hepatic cells. For example, gelatin-based hydrogels have been increasingly used to promote cell fate processes in 3D. Most gelatin-based systems require the use of physical gelation or non-specific chemical crosslinking. Both of these methods yield gelatin hydrogels with highly interdependent material properties (e.g., bioactivity and matrix stiffness). The purpose of this thesis research was to prepare modularly crosslinked gelatin-based hydrogels for studying the influence of independent matrix properties on hepatic cell fate in 3D. The first objective was to establish tunable gelatin-based thiol-norbornene hydrogels and to demonstrate that the mechanical and biological properties of gelatin hydrogels can be independently adjusted. Furthermore, norbornene and heparin dual-functionalized gelatin (i.e., GelNB-Hep) was prepared and used to sequester and slowly release hepatocyte growth factor (HGF). The second objective was to investigate the viability and functions of hepatocytes encapsulated in gelatin-based hydrogels. Hepatocellular carcinoma cells, Huh7, were used as a model cell type to demonstrate the cytocompatibility of the system. The properties of GelNB hydrogels were modularly tuned to systematically evaluate the effects of matrix properties on cell viability and functions, including CYP3A4 activity

and urea secretion. The last objective was to examine the effect of heparin immobilization on hepatocyte viability and functions. The conjugation of heparin onto GelNB led to suppressed Huh7 cell metabolic activity and improved hepatocellular functions. This hybrid hydrogel system should provide a promising 3D cell culture platform for studying cell fate processes.

1. INTRODUCTION

1.1 Liver, Disease, and 2D Culture of Hepatocytes

The liver is the largest organ in the body and is responsible for detoxification, metabolism, and protein synthesis. [1] Due to the presence of many cell types, the liver contains a very complex architecture (i.e., stellate cells, kupffer cells, hepatocytes, cholangiocytes, and mast cells). [2] Of the cell types found within the liver, hepatocytes are the major parenchymal cells that play crucial roles in liver functions. [1,3,4] Damages to hepatocytes can lead to hepatic diseases, including hepatitis, hepatocellular carcinoma, and cirrhosis. [1]

In 2011, liver disease was the twelfth-leading cause of death in the United States, contributing to nearly 11 deaths per 100,000 people. [5] Liver transplantation is the most common means of treating end stage liver failure; however, donors are in short supply, and many patients waiting to receive transplants experience death. [6] Recipients of transplanted livers experience recurring disease, or relapse, indicating a need to better understand the cause of disease. [6] An appropriate *in vitro* culture system is fundamental in understanding cell behavior and molecular signaling events involved in disease progression and repair mechanisms. [1]

Conventionally, two-dimensional (2D) cell cultures are employed to assess hepatocyte functions *in vitro*. However, when hepatocytes are cultured on two-dimensional (2D) tissue culture plastics (TCP), they typically experience abnormal proliferation profiles and suffer from loss of hepatocyte functions. [1,3,4] Additionally, hepatocytes cultured on 2D TCP do not experience appropriate cell-extracellular matrix (ECM) interactions and do not display natural polarity. [3] Due to the loss of liver-specific functions and a decrease in cell viability, drug screening applications are negatively impacted when hepatocytes are cultured in 2D. [4,7,8] Three-dimensional (3D) scaf-

folds recapitulating aspects of the natural ECM microenvironment should provide crucial cell-ECM interactions to maintain cell survival and functions. [9] As a result, there has been a paradigm shift in cell culture from 2D TCP to 3D biomaterials. [10]

1.2 Gelatin Based Hydrogels

Gelatin is a naturally derived protein hydrolyzed from fibrous collagen (type I). [11] The acidic hydrolysis of porcine skin results in type A gelatin with an isoelectric point (pI) of 8 and a net positive charge at a physiological pH of 7.4. On the other hand, the basic hydrolysis of bovine skin or bone results in type B gelatin possessing a pI of 5 and a net negative charge at pH 7.4. [12] Compared to its precursor, gelatin is more water soluble and has lower immunogenicity. [13] This property arises from gelatin's negligible quantities of aromatic amino acids tryptophan, phenylalanine, and tyrosine. As a result, antigenic reactions stimulated by aromatic radicals are less likely to form. [11]

Gelatin contains peptide sequences as binding sites (e.g., Arg-Gly-Asp sequence) for integrins and protease sensitive sites for matrix metalloproteinases (MMPs; specifically MMP-2 and MMP-9). [12–14] These domains allow cells to bind to and interact with the gelatin. Exploiting this property, gelatin has been used to modify materials that are otherwise inert to cells. [15] Gelatin in its unmodified form is considered to be a thermo-reversible biomacromolecule. Upon heating, gelatin can be dissolved into a viscous solution. Upon cooling to a temperature that is less than what is required for cell culture gelation occurs again. [12] Therefore, gelatin must be chemically modified to improve its stability in order to be used as a 3D culture system. [13]

Some researchers utilize small molecular weight crosslinkers such as genipin and glutaraldehyde to create gelatin hydrogels. For example, one group generated chitosan-gelatin scaffolds through crosslinking with glutaraldehyde to compare these scaffolds with alginate scaffolds. [16] Scaffolds without glutaraldehyde showed improved cytocompatibility verifying the enduring toxic effects of glutaraldehyde. [16] Due to the

toxicity of glutaraldehyde others have moved towards using the natural crosslinker genipin. Lau and colleagues crosslinked gelatin through reacting the primary amines of gelatin with genipin forming microspheres to function as hepatocellular microcarriers. [9] Although genipin has shown to have improved cytocompatibility over glutaraldehyde crosslinked constructs, genipin crosslinking of natural based structures (i.e., chitosan, alginate, collagen, gelatin, etc.) have lower mechanical properties. [17] Based on this, improved methods to generate increased mechanical properties while maintaining high levels of cytocompatibility are crucial in creating stable gelatin hydrogels for the culture of cells.

1.3 Chain-Growth Photopolymerization for Forming Covalently Crosslinked Gelatin Hydrogels

The crosslinking of hydrophilic polymeric networks creates hydrogels that are capable of imbibing large amounts of water. Hydrogels are permeable, which allows the diffusion of nutrients and oxygen. The polymerization mechanism (i.e., chain-growth polymerization or step-growth polymerization) affects the biophysical (e.g., stiffness) and biochemical (e.g., cell-responsive sights) properties of hydrogels. [18] Through modifying the amine groups of gelatin with methacrylic anhydride, methacrylamide groups were added onto the gelatin backbone creating a chemically modified form of gelatin (Figure 1.1). [19] Methacrylamide modified gelatin (i.e., GelMA) has allowed researchers to use chain-growth photopolymerization to form stable gelatin hydrogels useful for 3D cell culture, as well as soft and hard tissue regeneration. [20–26] For example, through a radically mediated polymerization, Anseth et al. and Khademhosseini et al. prepared GelMA hydrogels for *in situ* cell encapsulation and 3D cell culture. [27–29] In an effort to investigate hepatocyte viability and the restoration of hepatocellular functions, another group developed GelMA hydrogels with covalently immobilized galactose. [23]

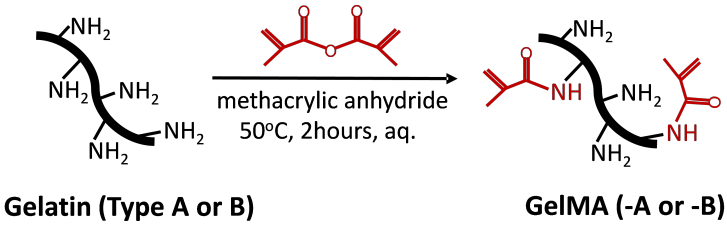

Fig. 1.1. Schematic of the synthesis of methacrylamide modified gelatin, or GelMA.

Although methacrylamide modified gelatin has proven to be useful when fabricated as a 3D cell culture platform, studies have shown that chain-growth photochemistries are less cytocompatible for radical-sensitive proteins and cells. [13, 30, 31] This is attributed to a high concentration of radical species and the long half-life of these radicals. [31, 32] In addition, the resulting heterogeneous network comprised of hydrophobic poly(methacrylamide) kinetic chains is not ideal for cell culture (Figure 1.3a). [13, 31] For chain-growth polymerized GelMA hydrogels, the elastic moduli, or stiffness, of gels are coupled to the network crosslinking density. To adjust stiffness, macromer concentration and/or the degree of macromer functionalization must be altered. [27, 28] Therefore, in order to tune the mechanical properties of GelMA hydrogels, gelatin concentration must be altered thereby altering the biological properties as well.

1.4 Step-Growth Thiol-Ene Photopolymerization for Forming Covalently Crosslinked Gelatin Hydrogels

Creating a 3D cell culture system that utilizes step-growth thiol-norbornene (or thiol-ene) photo-click chemistry will provide improved cytocompatibility and control over material properties. These improvements are a direct result of the photo-click reaction between thiol and ene moieties. Upon the exposure to light, thiyl radicals (generated from thiol containing crosslinkers) crosslink with ene moieties (Figure 1.2) to form a thiol-ene step growth polymerized network. The formation of thiol-

ene networks can be controlled both spatially and temporally and is non-oxygen inhibited. [13,31] In addition, thiol-ene photo-click hydrogels provide a more efficient immobilization of proteins/peptides and are suitable for creating a biomimetic microenvironment. [32, 33] Table 1.1 summarizes major advantages and disadvantages of different crosslinking methods used for gelatin hydrogels.

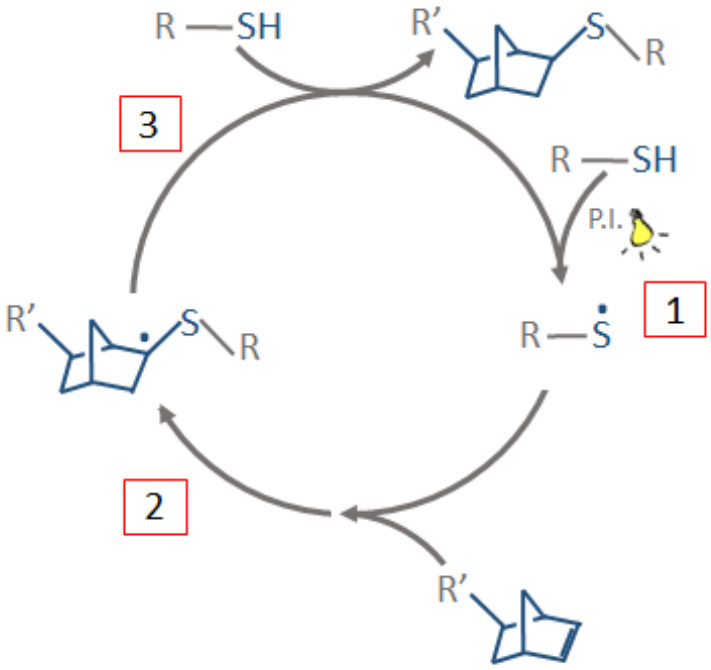

Fig. 1.2. Schematic of thiol-ene step growth polymerization. (1) Hydrogen atom is extracted from thiol group by initiating radical leading to the formation of a thiyl radical. (2) Thiyl radical associates with an ene functional group creating a carbonyl radical. (3) Chain transfer occurs between carbon radical and another thiol regenerating a thiyl radical, and the process repeats.

Our group has been interested in the biomedical applications of thiol-ene hydrogels formed by inert poly(ethylene glycol)-tetra-norbornene (PEG4NB) and simplistic protease sensitive bis-cysteine terminated peptides. Using this system, MIN6 β-cell viability was increased using step-growth thiol-ene photopolymerization over chain-

Table 1.1.
Chemical crosslinking methods used for gelatin hydrogels.

Crosslinking Method	**Advantages**	**Disadvantages**
Glutaraldehyde	• Very reactive	• Low cytocompatibility • Low mechanical strength
Genipin	• Natural • Cytocompatible • Very reactive	• Low mechanical strength
Chain-growth Photo-polymerization	• Increased mechanical properties	• Gelatin must be chemically modified • Oxygen inhibited • Radical-mediated damage • Heterogeneous hydrophobic kinetic chains • High-molecular-weight degradation products
Step-Growth Photo-polymerization (thiol-ene)	• Improved cytocompatibility • Increased spatial-temporal control in gelation kinetics • Requires fewer radicals for initiation • Rapid Gelation • Idealized and orthogonal network	• Gelatin must be chemically modified • Radical-mediated damage • Thiol groups react or denature proteins

growth photopolymerization.[31] In another study, we also reported orthogonal thiol-ene photochemistry using PEG4NB crosslinked by MMP-sensitive peptides enhanced

hepatocyte-specific genes and functions (i.e., NTCP, HNF4α, urea, CYP450) of Huh7 and HepG2 cells compared to PEG4NB crosslinked by DTT. Although proven to be cytocompatible, various biomimetic peptides were required to re-establish the complex cell-ECM interactions necessary to support cell fate processes *in vitro*. [4,34–36]

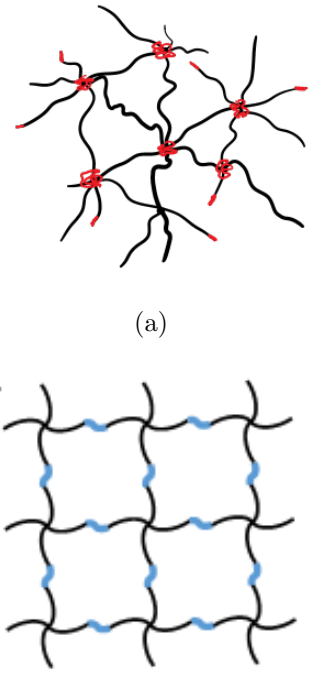

(a)

(b)

Fig. 1.3. Schematic of hydrogel network structure formed by: (a) Chain-growth photopolymerization. (b) Step-growth photopolymerization. (Items are not drawn to scale.)

To avoid the additional inclusion of synthetic peptides, our group synthesized orthogonally crosslinked gelatin based hydrogels from norbornene-functionalized gelatin (GelNB) and multifunctional-thiol crosslinker. [13] Mechanical properties of GelNB hydrogels could be tuned through a multitude of methods such as adjusting macromer concentration, crosslinker concentration, or by adjusting the functionality of the crosslinker. For example, a higher degree of network crosslinking could be achieved without changing the concentration of GelNB but through replacing bi-functional dithiothreitol (DTT) with tetra-functional PEG-thiol (PEG4SH). GelNB hydrogels

crosslinked by thiol containing crosslinkers were cytocompatible with human mesenchymal stem cells (hMSCs). Comparing hydrogels prepared by step-growth polymerization with hydrogels prepared by chain-growth polymerization a greater extent of cellular interaction can be seen. Differences in cellular interaction are a direct result of the networks created by the specific chemistries. Step-growth polymerization allows the formation of orthogonal (1 to 1 reaction of thiol to ene moieties) crosslinks in GelNB gels (Figure 1.3b); whereas chain-growth chemistry leads to the creation of heterogeneous poly(methacrylamide) kinetic chains in hydrogels formed by GelMA (Figure 1.3a). [30,31] While GelNB hydrogels crosslinked by thiol containing crosslinkers have proven cytocompatible, the modification of GelNB with additional bioactive motifs (e.g., heparin), which may further impact cell fate processes, especially for hepatic cells, has not yet been reported.

1.5 The Role of Heparin within the Liver and on Hepatocytes

Heparin is a highly sulfated and negatively charged glycosaminoglycan (GAG) found in abundance in the liver and is capable of sequestering growth factors as well as protecting them from proteolysis. [37–41] Mast cells of the liver are responsible for the synthesis of heparin and other cytokines, chemokines, proteases. These cells are located in proximity of vasculature walls or in close association with the surrounding connective tissues of vessels. [42] This ideal location assists in the distribution of inflammatory responses mediated by mast cells during inflammatory events or injury. The most commonly known medical use of heparin is for anti-coagulation. In the liver, heparin has been identified in the sequestering of hepatocyte growth factor (HGF). Together, heparin and HGF form a complex that aids in hepatocytes expressing necessary liver functions such as albumin production, CYP function, and urea secretion. [38, 43, 44]

To investigate the effect of heparin on hepatocytes, many researchers have utilized heparin in conjunction with synthetic polymers for the cultivation of hepatocytes in

2D as well as 3D. You and associates created multi-layered heparin/PEG microwells for enhancing hepatocyte function. [40] Rat primary hepatocytes cultured in microwells coated with heparin presented cuboidal morphology indicative of a natural hepatocyte phenotype. Cells cultured in heparin-containing microwells expressed more urea and albumin compared to those cultured in wells without heparin. Kim et al. prolonged the cultivation of rat primary hepatocytes with the inclusion of thiolated heparin within PEG-diacrylate (PEGDA) hydrogels formed by Michael-type addition chemistry. [37] The incorporation of heparin within PEG hydrogels improved the viability and hepatocyte-specific functions (i.e., albumin and urea secretion) of the encapsulated cells. In the same study, the growth factor sequestering effect of heparin was examined through the sustained release of HGF. [37]

Instead of using inert PEG, others have conjugated heparin onto natural materials such as collagen and gelatin in order to study heparin's influence on neighboring cells and/or the sequestering of growth factors. Hou and colleagues developed a HGF/heparin immobilized collagen system with which they could quantify albumin synthesis and investigate hepatocyte morphology. [45] The presence of heparin enhanced the synthesis of albumin but had no effect on the morphology of rat primary hepatocytes. Nakamura et al. reported the conjugation of heparin to gelatin through a Borch reaction between aldehyde-modified heparin and the amino groups of gelatin. [38] Li and associates utilized standard 1-ethyl-3-(3-dimethylaminopropyl)carbodiimide (EDC) and N-hydroxysuccinimide (NHS) chemistry to conjugate heparin onto tyramine modified gelatin in order to evaluate growth factor immobilization and its effect on angiogenesis. [46] Regardless of how heparin was incorporated, its inclusion enhanced growth factor performance and hepatocyte function.

2. OBJECTIVES

2.1 Prepare Modularly Crosslinked Gelatin Hydrogels with Heparin Immobilization

The first objective of this thesis was to utilize thiol-ene photochemistry to create gelatin based hydrogels with independently tunable mechanical and biological properties. Through adjusting either macromer concentration or the ratio of thiol to norbornene moieties, the mechanical and biological properties of thiol-ene hydrogels were easily controlled. In addition, heparin was immobilized within gelatin based hydrogels, and its effect on stiffness and growth factor sequestering was investigated. Results obtained here provide the ground work for subsequent studies of hepatic cell fate in 3D.

2.2 Investigate Hepatic Cell Viability and Functions in Modularly Crosslinked Gelatin hydrogels

After establishing a tunable gelatin based hydrogel platform, the second objective was to evaluate the viability and hepatocellular functions of Huh7 cells cultured in 3D. Metabolic activity, CYP enzyme activity, and urea secretion were monitored. Additionally, cell viability was investigated through live/dead staining of cells. The purpose of these studies is to investigate whether our platform provides relevant mechanical and/or biological properties that will support the survival and function of hepatic cells.

2.3 Examine the Effect of Heparin Immobilization on Hepatic Cell Viability and Functions in 3D

The third objective of this thesis was to evaluate the viability and hepatocellular functions of Huh7 cells in heparin immobilized thiol-ene gelatin based hydrogels. Cell viability was investigated through metabolic activity and live/dead staining of cells. Additionally, hepatocellular functions such as CYP enzyme activity and urea secretion were examined. These results provide information regarding the utility of this hydrogel platform as a 3D culture for hepatic cells.

3. MATERIALS AND METHODS

3.1 Materials

Type A gelatin (Bloom 238282) and type B gelatin (Bloom 225) were obtained from Amresco, and Electron Microscopy Sciences, respectively. 4-arm PEG-OH (M.W. 20 kDa) and 4-arm PEG-SH (M.W. 10 kDa) were purchased from JenKem Technology USA. AlamarBlue reagents were purchased from Thermo Scientific. Urea assay and CYP3A4 assay were purchased from BioAssay Systems and Promega, respectively. Live/Dead staining kit for mammalian cells was acquired from Life Technologies Corp. DPBS, fetal bovine serum (FBS), 100 antibioticantimycotic, and DMEM were acquired from HyClone. Heparin sodium salt was obtained from Akron Biotech. 1-Ethyl-3-(3-dimethylaminopropyl) carbodiimide (EDC) and N-Hydroxysuccinimide (NHS) were obtained from Fisher and TCI chemicals, respectively. Recombinantmurine HGF and ELISA kit were procured from Peprotech and R&D systems, respectively. Bromocresol green sodium salt was purchased from Alfa Aesar. 1,9-Dimethyl-methylene Blue (DMMB) zinc chloride and all other chemicals were obtained from Sigma-Aldrich unless otherwise noted.

3.2 Synthesis of Gelatin Based Macromers

GelNB was synthesized by reacting gelatin with carbic anhydride as previously published by our group. [13] At 50°C, 10 wt% gelatin was added to a round bottom flask containing PBS (pH 7.4) and stirred. Once the gelatin dissolved, carbic anhydride (20wt/vol%) was slowly added to the solution while the pH was adjusted using a solution of sodium hydroxide. After 72 hours of reaction time, 3X warm PBS (37°C) was added to halt the reaction. The solution was then centrifuged to rid the

solution of any unreacted or undissolved carbic anhydride. Following centrifugation, the GelNB solution was dialyzed against 40°C ddH_2O for 3 days (MWCO: 6-8 kDa) and lyophilized to retrieve final dry product. The degree of norbornene substitution was determined with fluoraldehyde assay using unmodified gelatin with known concentrations as standards (D.S. ∼2.2 mM ene per 1 wt% of gelatin; for both type A and type B). GelNB-Hep was synthesized using standard EDC/NHS chemistry [46,47] but with GelNB as the starting material. Briefly, heparin (1 wt/vol%) was dissolved in ddH_2O and the concentration of carboxyl groups on heparin was determined by bromocresol green assay. To the heparin solution, 10x molar excess of EDC and NHS were added for the activation and stabilization of carboxyl groups on heparin and was stirred for 30 minutes at room temperature to allow the reaction to occur. In another vessel, GelNB (∼2.5 wt/vol%) was dissolved in ddH_2O and added to the activated heparin solution. The reaction was allowed to proceed for another 18 hours at room temperature with gentle stirring. After which, the GelNB-Hep solution was collected and dialyzed (MWCO of dialysis membrane: 6-8 kDa) against 0.2M NaCl for 72 hours, followed by another dialysis in ddH_2O for 72 hours. The dialyzed samples were lyophilized and the degree of heparin substitution (D.S.) was determined with DMMB assay using unmodified heparin at known concentrations as a standard (D.S. ∼0.003 wt% heparin per 1 wt% of GelNB).

3.3 Hydrogel Fabrication

Thiol-norbornene hydrogels were created by radical-mediated step-growth photopolymerization. Macromers gelatin-norbornene (GelNB) and poly(ethylene glycol)-tetra-norbornene (PEG4NB, 20kDa) were reacted with gel cross-linker and co-initiator Poly(ethylene glycol)-tetra-thiol (PEG4SH, 10kDa)) to form a crosslinked hydrogel. The molar ratio between thiol and ene groups (R) was adjusted to achieve numerous hydrogel formulations. Aliquots of pre-polymer solutions were injected into glass slides separated by 1 mm Teflon spacers and utilizing an ultra violet light-mediated

thiol-ene photopolymerization with the primary initiator lithium acylphosphinate (LAP, 1 mM) hydrogels were fabricated. Pre-polymer solutions, for all hydrogels, was subjected to 365 nm light at an intensity of 5mW/cm^2 for 5 minutes.

3.4 Rheometry

A Bohlin CVO 100 digital rheometer was used to probe *in situ* gelation kinetics and to investigate rheological properties. To form gels for rheometry, aliquots of pre-polymer solutions were injected into glass slides separated by 1 mm Teflon spacers. Following gelation, disc-shaped hydrogels were punched with an 8 mm diameter biopsy punch. Moduli of the gels were measured using parallel plate with gap size of 800 μm. Oscillatory rheometry was operated in strain sweep mode (0.1% to 5% strain) at a frequency of 1 Hz and averaged G' values were obtained from the linear portion of the modulus-strain curves. A light cure cell was further used to probe the *in situ* gelation kinetics of thiol-ene gelatin hydrogels at room temperature. On top of a quartz plate within the light cure cell, the pre-polymer solution (100 μL) was placed and exposed to UV light (Omnicure S1000. 365 nm, 5 mW/cm^2).

3.5 Proteolyitic Degradation

After photopolymerization of hydrogels following the method described previously, the initial mass of hydrogels was measured, and then gels were placed in wells containing 1 mL of PBS containing chymotrypsin (1mg/mL). Gels were incubated at room temperature on an orbital shaker. Every 10, 15, or 30 minutes, gels were removed from protease solution, blotted dry, mass was recorded, and returned to incubate in the chymotrypsin solution. This process was repeated until the gel itself had completely degraded. Every 30 minutes the chymotrypsin solution was refreshed to ensure enzyme activity. Results were presented as percent mass loss, and percent mass loss is defined as: Mass loss (%) = ((W_t - W_0) / W_0) x 100%, where W_t is the hydrogel weight measured at specified time points and W_0 is the initial mass measured.

3.6 Immobilization of Heparin and *In Vitro* HGF Release from GelNB Hydrogels

As briefly mentioned, the degree of heparin substitution onto GelNB was determined (∼0.003 wt% Heparin per 1 wt% of GelNB) with the dimethyl-methylene blue assay using unmodified GelNB with known concentrations as standards. DMMB was further used as a qualitative reagent to detect the immobilization of heparin within GelNB hydrogels. After thiol-ene gelation, hydrogels (pure PEG, 1% GelNB-A/B, or 1% GelNB-A/B-Hep) were washed in PBS (pH 7.4) for 1 hour to allow un-crosslinked elements to be leached from the gel. Following one hour, gels were moved to a 2 mL bath of DMMB and allowed to incubate at room temperature for nearly 24 hours. After which, gels were then transferred to PBS to remove remaining DMMB solution within the network. Once gels were washed in PBS for 24 hours, images were captured.

7 wt% of type A GelNB or GelNB-Hep hydrogels were prepared as described earlier but the gels were loaded with 200 ng/gel of recombinant mouse HGF. After gelation, gels were submerged in 5mL of release buffer composed of 0.1 wt% BSA and kept at 37°C. At pre-determined time periods, 400 μl of solution samples were collected and the buffer was reconstituted to 5 ml with fresh release buffer. Immediately following collection the samples were stored at -80°C until analysis with HGF ELISA kit (DuoSet ELISA mouse HGF kit, R&D Systems). In brief, a 96-well clear microplate was coated with 100 μL/well of capture antibodies without protein carriers (goat anti-mouse HGF, 0.8 μg/mL in PBS). The plate was sealed and allowed to incubate over night at room temperature. Following a series of 3 washes using wash buffer (0.05% Tween in PBS pH 7.4), the wells were blocked by adding 300 μL reagent diluent (1wt% BSA in PBS pH 7.4, filtered) to each well. After 1 hour incubation, covered, at room temperature, the reagent diluent was removed from the plate and 100 μL of the collected samples and HGF standard were added and allowed to incubate covered at room temperature for 2 hours. Again, after a series of 3 washes with

wash buffer, 100 μL of detection antibody (biotinylated goat anti-mouse HGF, 200 ng/mL in reagent diluent) was added to each well and incubated at room temperature for an additional 2 hours. Following, the plate was washed again and 100 μL of a working solution of streptavidin conjugated horseradish-peroxidase was added to each well. After 20 minutes incubation at room temperature the plate was washed a final time. While avoiding direct sunlight, the plate was incubated at room temperature for 20 minutes after the addition of 100 μL of substrate solution (1:1 mixture of Color Reagent A (H_2O_2) and Color Reagent B (Tetramethylbenzidine)) per well. Upon the expiration of time, 50μL/well stop solution (2N H_2SO_4) was added to the plate and the absorbance was immediately read at 450 nm.

3.7 Cell Culture

Human derived immortalized hepatocarcinoma cells (Huh7) (courtesy of Dr. Guoli Dai Biology Department, IUPUI) were maintained in high glucose DMEM (Hyclone) augmented with 10% fetal bovine serum (FBS) (Gibco) and 1x antibioticantimycotic (Invitrogen, 100 U/mL penicillin, 100 μg/mL streptomycin). Culture media were refreshed every 2-3 days.

3.8 Cell Encapsulation

Following a procedure similar to that performed for hydrogel fabrication, cell encapsulation was achieved. Upon suspending cells (used at a final cell density of $5x10^6$ cells/mL) in a sterile polymer precursor solution containing the desired concentration of GelNB/PEG4SH or GelNB/PEG4NB/PEG4SH with 1mM LAP (photo-initiator) for every 20 μL of precursor solution, cell encapsulation as well as hydrogel formation were concurrently completed through exposure to long-wave ultra violet light (365 nm, 5 mW/cm^2) for 5 min at room temperature. Succeeding cell encapsulation, cell-laden hydrogels were maintained in Huh7 growth media (high-glucose DMEM,) and cultured at 37°C in 5% CO_2. Culture media were refreshed every 2-3 days.

3.9 Cell Viability and Functional Assays

To investigate cell viability within hydrogels qualitatively, encapsulated HUH7 cells were incubated in a solution containing Live/Dead stain (Life Technologies) and imaged with a confocal microscope (Olympus Fluoview FV100 laser scanning microscope). Z-stack images (100 μm thick, 10 μm per slice) from one gel and of at least three random fields were captured for all experimental conditions. On Day-0, live (green) and dead (red) cells were counted in each of the three captured images and the viability was determined by normalizing the number of live cells to the total number of cells. For each group, total number of cells ranged from about 140-280 cells.

Cell metabolic activity was evaluated to investigate the long-term viability and proliferation of encapsulated cells via incubating the cell-laden hydrogels in Alamar-Blue reagent (1:10 dilution in cell culture media) for 90 minutes. Following incubation, 200 μl samples of media were transferred to a clear 96-well plate. Using a microplate reader, the changes in fluorescence were read (excitation: 560 nm, emission: 590 nm).

Hepatocyte-specific functions in the encapsulated cells, including urea secretion and CYP3A4 enzymatic activity, were measured post-encapsulation. The cell culture media were refreshed 48 hours prior to sampling and the collected media samples were analyzed for urea content using a commercially available urea assay kit (QuantiChrom Urea assay kit, Bioassay systems). In brief, 50 μL of collected samples, urea standard, and media blank were added to a white 96-well plate. After which, 200 μL/well of working reagent (1:1 ratio of Reagent A and Reagent B) were mixed with plated standards and samples and were allowed to incubate for 20 minutes. Following the incubation period, the optical density was measured via a microplate reader (430 nm).

CYP3A4 enzyme activity assay was performed using P450-Glo CYP3A4 Lucifierin-IPA kit (Promega). Using a 48-well plate, 300 μL of culture media containing 3 μM luciferin IPA to each well. Gels were then transferred to individual wells and allowed

to incubate for 60 minutes at 37°C. Following incubation, gels were transferred back into original culture plates, and 50 μL samples of IPA-media were transferred from the 48-well plate to a white 96-well plate individual already containing 50 μL of luciferin detection reagent per well. The two components were allowed to incubate at room temperature for 20 minutes. Immediately following the 20 minutes, the luminescence was read using a microplate reader (2D samples were scaled to high whereas media blanks were scaled to low). Urea secretion and CYP3A4 activity levels were normalized by the cell metabolic activity from the respective cell-laden hydrogel in an effort to offset variances in metabolic activity so that cell functions may be investigated independently of metabolic activity.

3.10 Statistics

All experiments were conducted independently for at least three times. Each experimental or control group contained at least three samples. Results were presented as Mean ± SD. 2-way ANOVA and when permitting a Bonferroni post-test was performed to evaluate the statistical significance between indicated groups (* denote $p < 0.05$, ** denote $p < 0.001$, *** denote $p < 0.0001$).

4. RESULTS AND DISCUSSION

4.1 Prepare Modularly Crosslinked Hydrogels with Heparin Immobilization

Step-growth photopolymerized GelNB hydrogels can be mechanically tuned by holding gelatin content constant and adjusting only the concentration of crosslinker. Conversely, biologically tunable properties can be achieved through holding the stiffness constant while the gelatin content is adjusted. The ability to independently tune biophysical and biochemical properties can be used to gain a better understanding of the influence of ECM cues on cell processes.

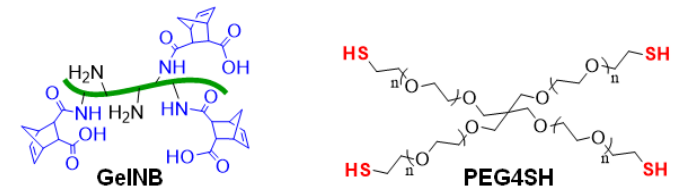

(a)

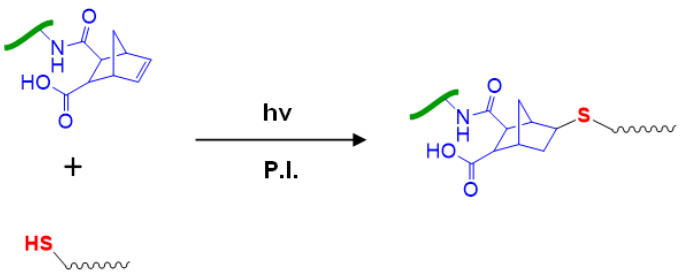

(b)

Fig. 4.1. (a) Chemical structures of norbornene-functionalized gelatin (GelNB) and PEG-tetra-thiol (PEG4SH). (b) Light and radical mediated thiol-norbornene photo-click reaction.

Norbornene-functionalized gelatin had to first be synthesized. This was achieved through reacting carbic anhydride with unmodified gelatin. The resulting degree of norbornene substitution was determined by using fluoraldehyde assay to quantitatively assess the amount of amine groups present on gelatin's backbone before and after the reaction. No matter the type of gelatin, ∼2.2 mM ene was successfully conjugated per 1 wt% of gelatin.

To investigate the effect of GelNB macromer content and thiol-to-ene molar ratio (R) on light-mediated orthogonal thiol-norbornene gelation, we conducted gelation studies using *in situ* photorheometry. Macromer GelNB and crosslinker PEG4SH (Figure 4.1a) were used to form gelatin hydrogels with orthogonal thiol-ene crosslinks (Figure 4.1b).

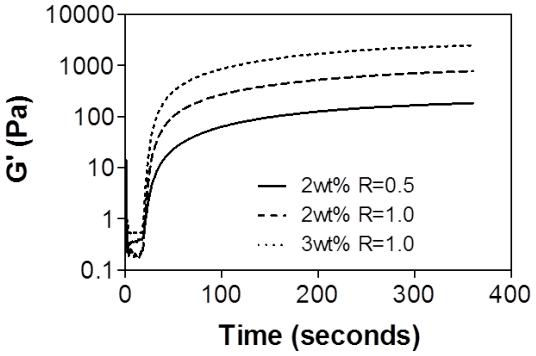

Fig. 4.2. *In situ* photorheometry of GelNB-A using PEG4SH as crosslinker. Light was turned on 10 seconds after initiating the measurements. Inlet image shows a representative gelatin based thiol-ene hydrogel.

Precursor solutions begin to gel very rapidly upon exposure to 365 nm light at an intensity of 5 mW/cm^2. As shown in Figure 4.2, increased [GelNB] from 2wt% to 3wt% or increased R from 0.5 to 1 did not change gel point significantly (∼6-8 seconds). However, gels formed by higher [GelNB] or higher R yielded higher stiffness (Table 4.1, formulations A-C). The rapid gel points of GelNB hydrogels can be attributed to the rapid radical-mediated photopolymerization, the non-oxygen-

inhibited thiol-norbornene reaction, as well as the presence of multiple norbornene functionalities on a single GelNB macromer.

Table 4.1.
Hydrogel formulations used in Figures 4.2 and 4.3.

	GelNB		**$PEG4SH_{10kDa}$**		
	wt%	**[ene](mM)**	**wt%**	**[thiol](mM)**	**$Ratio_{[thiol]/[ene]}$(R)**
A	2	4.4	0.6	2.2	0.5
B	2	4.4	1.1	4.4	1.0
C	3	6.7	1.7	6.7	1.0

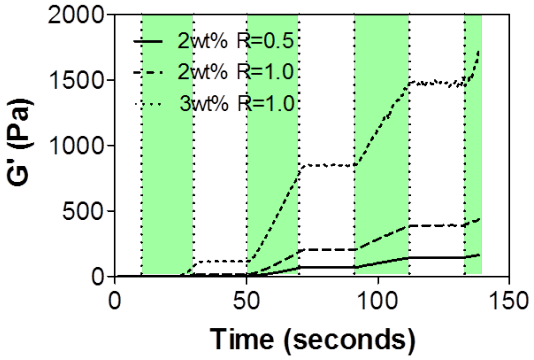

Fig. 4.3. Temporal control of thiol-ene gelation using intermittent light exposure. Shaded regions represent the presence of light.

Because gelatin can gel physically, it is crucial to verify that the formation of GelNB hydrogels is a result of light-mediated thiol-ene gelation. Here, pre-polymer solutions were subjected to alternating rounds of light exposure (i.e., alternating light exposure and darkness for at least 3 cycles) during *in situ* rheometry (Figure 4.3). One can see that gel modulus only increased in the presence of light and leveled off immediately upon switching off the light, indicating that hydrogel crosslinking

was indeed a result of light-mediated thiol-ene photopolymerization and not physical gelation.

4.1.1 Result of Macromer Concentration on Stiffness and Degradation

The mechanical property of the GelNB hydrogel was tuned by adjusting the concentration of bio-inert macromers (i.e., PEG4NB or PEG4SH) in the precursor solution (Table 4.2, formulations B, D-H). Results shown in Figure 4.4 demonstrate that, at a fixed concentration of GelNB (i.e., 2 wt%), or bioactive motifs, hydrogel shear moduli increased (∼0.8 kPa to ∼8 kPa) with increasing concentrations of bio-inert crosslinkers for both types of GelNB. This signifies the ability to tune the mechanics while maintaining constant biological properties. Additionally, Table 4.3 demonstrates the independent control of gelatin content (1-7 wt%), or biological properties, without significantly affecting gel stiffness, or mechanics. This allows the concentration of bioactive motifs to be adjusted while maintaining a similar crosslinking density in all groups.

Table 4.2.
Hydrogel formulations used in Figure 4.4.

	GelNB		**PEG4NB$_{20kDa}$**		**PEG4SH$_{10kDa}$**		
	wt%	**[ene](mM)**	**wt%**	**[ene](mM)**	**wt%**	**[thiol](mM)**	**R**
B	2	4.4	0	0	1.1	4.4	1.0
D	2	4.4	0.20	0.4	1.2	4.8	1.0
E	2	4.4	0.45	0.9	1.3	5.3	1.0
F	2	4.4	0.58	1.2	1.4	5.6	1.0
G	2	4.4	1.13	2.3	1.7	6.7	1.0
H	2	4.4	1.68	3.3	1.9	7.7	1.0

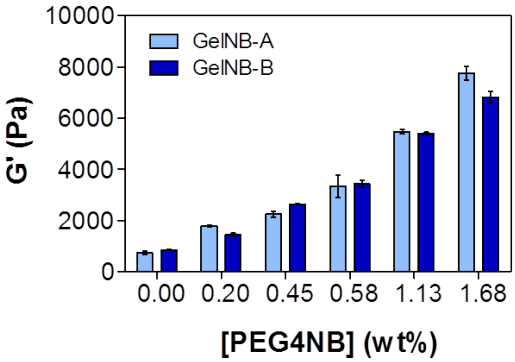

Fig. 4.4. Fine-tuning the crosslinking density through altering concentrations of macromer (GelNB, PEG4NB, or PEG4SH). At a constant gelatin content (2wt%) hydrogel crosslinking density could be tuned by adjusting PEG4NB and PEG4SH (Table 4.2 compositions B, D-H) while maintaining a constant ratio of mM thiol per mM ene (R = 1).

Table 4.3.
Hydrogel formulations used to tune gelatin content without significantly affecting hydrogels stiffness.

	GelNB		**PEG4NB$_{20kDa}$**		**PEG4SH$_{10kDa}$**		
	wt%	**[ene](mM)**	**wt%**	**[ene](mM)**	**wt%**	**[thiol](mM)**	**G' (Pa)**
I	1	2.2	1.0	2.0	1.05	4.2	2.0±0.76
J	3	6.7	0	0	1.2	4.8	2.2±0.13
K	5	11	0	0	0.9	3.7	2.1±0.95
L	7	15.4	0	0	0.85	3.4	2.0±0.42

To understand the protease degradability of orthogonally crosslinked GelNB hydrogels, we conducted proteolytic degradation studies using chymotrypsin as a model enzyme. While collagenase or gelatinase can be used to degrade gelatin hydrogel, we chose to use chymotrypsin since it is a more economical option and can achieve similar proteolytic gel degradation. [31] Chymotrypsin cleaves C-terminal peptide bonds fol-

lowing large hydrophobic amino acids like tyrosine, proline, and tryptophan. Gelatin contains high proportion of proline and some tyrosine, both of which are substrate for chymotrypsin-mediated cleavage. [12, 31, 48]

One method to modularly tune the crosslinking density of orthogonal gelatin hydrogels is through adjusting macromer concentration. GelNB hydrogels were formed with different concentrations (3, 5, 7 wt%) at a unity of R. At a fixed R-value (i.e., R = 1), gels could be easily prepared with a wide range of stiffness (i.e., ∼5 kPa to ∼20 kPa) through adjusting the gelatin content (Figure 4.5, Table 4.4 formulations C, M-N). Clearly, gel moduli increase at higher weight contents of GelNB or higher R-values.

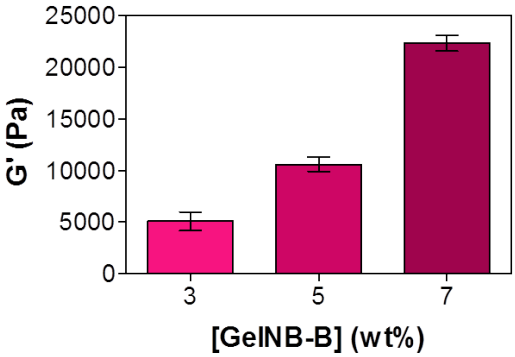

Fig. 4.5. Fine-tuning the crosslinking density through altering the concentration of gelatin. At a fixed R-value, crosslinking density can be tuned by varying the amount of macromer GelNB (Table 4.4 compositions C, M, N).

Within 3 hours of chymotrypsin treatment, all GelNB hydrogels eroded (Figure 4.5). Interestingly, hydrogel degradation mode seemed to be influenced by the initial gel crosslinking density. Specifically, the weights of hydrogels formed with 5 and 7 wt% GelNB increased (i.e., negative % in mass loss) during the initial hours of chymotrypsin treatment (Figure 4.6). These hydrogels also appeared to swell in size during the first one to two hours of protease treatment, indicating that the degradation had happened throughout the hydrogel network and in turn the gels

Table 4.4.
Formulations and initial moduli of hydrogels used in Figures 4.5-4.8.

	GelNB		$PEG4SH_{10kDa}$			
	wt%	**[ene](mM)**	**wt%**	**[thiol](mM)**	**R**	**G' (Pa)**
C	3	6.7	1.7	6.7	1	4.9±0.12
M	5	11	2.7	11	1	10.6±0.70
N	7	15.4	3.8	15.4	1	22.0±0.75
O	7	15.4	1.9	7.7	0.5	6.7±0.34
P	7	15.4	2.9	11.5	0.75	14.2±0.37

imbibed more protease solution, leading to a gain in gel mass. After a sufficient amount of gelatin molecules were cleaved, the gel mass started to decrease (positive in mass loss) and the gels eventually lost their structural integrity. On the other hand, gelatin hydrogels formed at 3 wt% started to lose mass immediately upon placing gels in chymotrypsin solution. The gels also appeared thinner as the enzyme cleaved the gels from the exterior through a surface erosion mechanism. This process continued until the entire hydrogel disappeared.

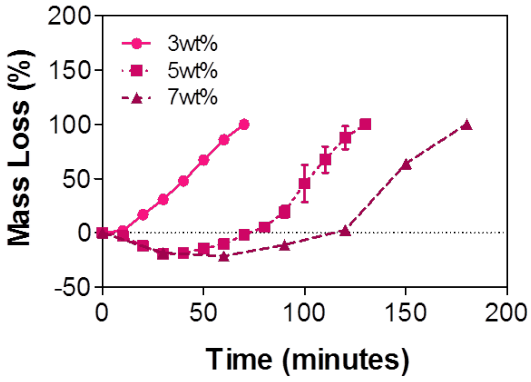

Fig. 4.6. Chymotrypsin-mediated (2mg/mL) proteolysis and mass loss of GelNB hydrogels crosslinked at different GelNB content.

These experiments demonstrated the ability to modularly control the mechanical (e.g., crosslinking density and stiffness) and biological properties (e.g., cell adhesiveness and protease sensitivity) of the cell-laden GelNB hydrogels.

4.1.2 Effect of Thiol to Ene Ratio on Stiffness and Degradation

Another method to modularly tune the crosslinking density of orthogonal gelatin hydrogel is through adjusting R, the molar ratio of thiol to norbornene groups. At a fixed gelatin content (i.e., 7 wt% GelNB-B), again, gels could be easily prepared with a wide range of stiffness (i.e., ∼6 kPa to ∼20 kPa) by simply adjusting R from 0.5 to 1 (Figure 4.7, Table 4.4 formulations N-P).

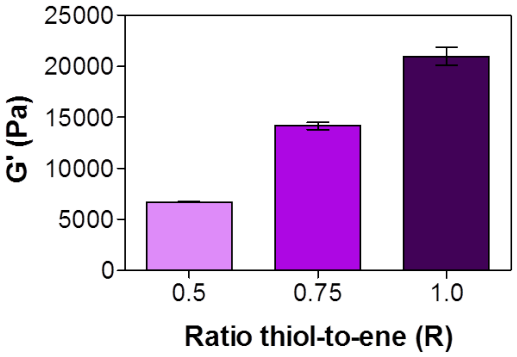

Fig. 4.7. Fine-tuning the crosslinking density through altering concentrations thiol to ene ratio. At a fixed GelNB-B content (7wt%) crosslinking density can be tuned by varying the ratio of mM thiol per mM ene via adjusting only the crosslinker PEG4SH (Table 4.4 compositions N-P).

Similar to controlling the weight percent of GelNB, altering the R-value also dictates how GelNB hydrogel is degraded proteolytically. As shown in Figure 4.8, all GelNB hydrogels eroded within 4 hours but hydrogels formed at R = 0.5 and 0.75 degraded faster and with a surface-erosion mechanism (enzyme cleaves gels from the exterior). On the other hand, gels formed at R = 1 degraded slower and in a bulk degradation mechanism (enzyme cleaves gels from the inner network). These results

suggest that when the crosslinking density of GelNB hydrogels is low, the cleavage of gelatin chains by protease leads to easy removal of gel fragments and the degradation exhibits a typical surface erosion mechanism. On the other hand, when the crosslinking density of GelNB hydrogels is high, initially most of the protease-cleaved gelatin chains are still attached to the network because of the high amount of crosslinks. This leads to the infiltration of more protease into the gel network that causes increased network cleavage and water uptake (hence the increase in gel mass), and eventually the loss of gel integrity. The variation in degradation mechanisms may be explored for delivering growth factors in a dynamic fashion. Additionally, these experiments further demonstrate this platform's ability to be independently tuned mechanically and biologically.

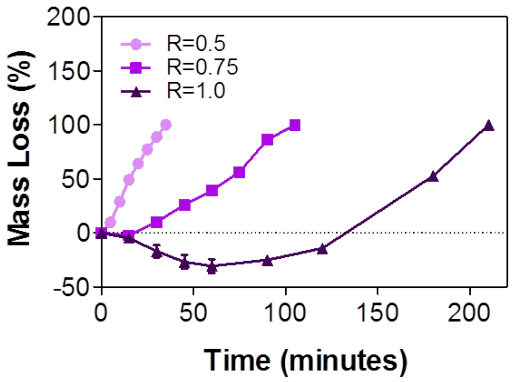

Fig. 4.8. Chymotrypsin-mediated (2mg/mL) proteolysis and mass loss of GelNB hydrogels crosslinked at different thiol-to-ene ratios.

4.1.3 Detection of Heparin Immobilization and Its Effect on Stiffness

Heparin, a highly sulfated and negatively charged glycosaminoglycan, acts as reservoir for matrix proteins and is abundant in the liver indicating that its use in recreating a liver cell's native environment may be important. [41] To immobilize heparin within the modularly crosslinked gelatin hydrogels, we synthesized a hep-

arin modified form of GelNB (GelNB-Hep, Figure 4.9a) through standard EDC/NHS chemistry (refer to section 3.2). Heparin conjugation onto GelNB was qualitatively assessed by dimethyl-methylene blue (DMMB) assay (Figure 4.9b).

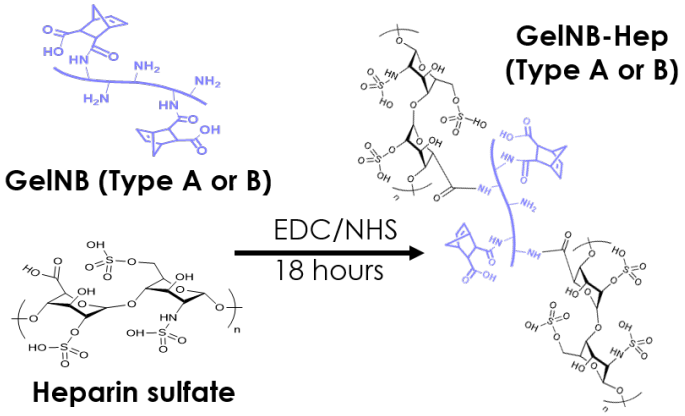

(a)

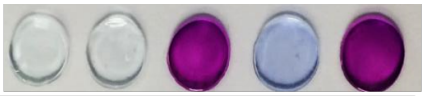

GelNB	-	A	-	B	-
GelNB-Hep	-	-	A	-	B

(b)

Fig. 4.9. (a) Schematic of heparin conjugated gelatin-norbornene (GelNB-Hep) synthesis. (b) Dimethyl methylene blue (DMMB) qualitative assay to verify immobilization of heparin within hydrogels. All gels contained 1.7 wt% PEG4NB and 1.4 wt% PEG4SH except type A and B gelatin which include an additional 1 wt% of gelatin.

DMMB possesses a positive charge and as a result binds to sulfated polysaccharides. Once bound DMMB undergoes a colorimetric change from blue to purple/pink. Clearly, gels containing no gelatin appeared transparent since no DMMB was able to bind to the non-charged PEG hydrogel. Similarly, gels made with GelNB-A also appeared transparent; whereas, hydrogels containing GelNB-B appeared blue in color. Gels containing heparin (GelNB-A-Hep and GelNB-B-Hep), on the other hand, appeared dark pink in color, suggesting that the immobilized heparin was able to react

with the DMMB dye as it infiltrated the hydrogels. Additionally, as mentioned previously the two types of gelatin possess different charges as a result of dissimilar processing techniques. Type A gelatin is positively charged, and type B gelatin is negatively charged. Therefore, the blue color obtained by the hydrogel including GelNB-B is a result of electrostatic interactions between the negative charge of GelNB-B and the positive charge of DMMB.

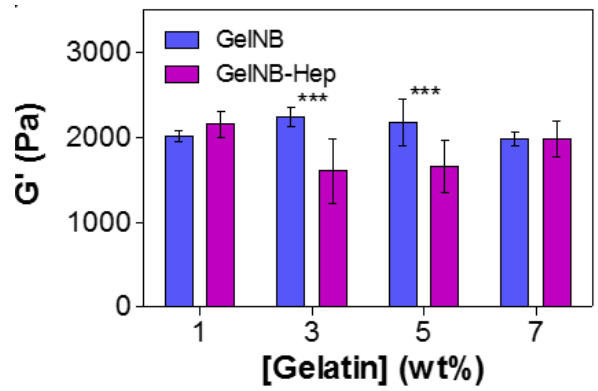

(a)

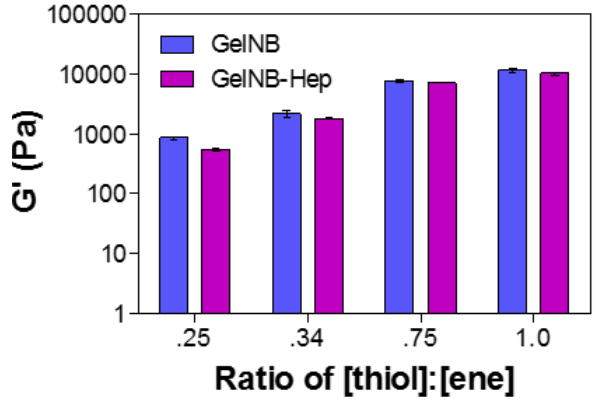

(b)

Fig. 4.10. (a) Effect of heparin immobilization on hydrogel stiffness at different gelatin content (type B: 1, 3, 5, 7 wt%). (b) At a fixed gelatin content (5 wt%) hydrogel stiffness more closely matches with increasing thiol to ene ratio (R).

Further investigating the effect of heparin conjugation onto GelNB, hydrogel moduli was re-evaluated. As depicted in Figure 4.10a, heparin incorporation affected gels containing 3 and 5 wt% GelNB-Hep to a greater degree than gels containing the extreme concentrations of gelatin when compared to GelNB hydrogels of matching formulations (**$p < 0.001$). However, 1 and 7 wt% GelNB-Hep hydrogels crosslinking efficiency was not hindered. The stiffness of hydrogels comprised of only 1 wt% gelatin was not affected by heparin due to the miniscule amount actually incorporated ($\sim$0.003 wt% Heparin). Heparin's large size possibly interfered with the crosslinking of 3 and 5 wt% hydrogels. Further experiments were conducted on 5 wt% gels using different R-values to explore the mechanism behind heparin's effect on stiffness. As the ratio of thiol-to-ene was increased discrepancies in moduli decreased as shown in Figure 4.10b. This relationship may derive from the negatively charged environment created by type B gelatin assisting in the deprotonation of increasing thiol moieties therefore increasing the crosslinking efficiency of hydrogels. Formulations for 7 wt% GelNB hydrogels may contain a sufficient amount of thiol and gelatin to create the increased effect of negative charge on deprotonation. It may also be likely that at 7 wt% GelNB there exists an increase in the spatial arrangement of ene moieties positioned along the gelatin backbone. This increase may allow more room to accommodate the large heparin molecules preventing the hindrance of crosslinking induced by heparin.

4.1.4 Sequestering of Hepatocyte Growth Factor

To exploit heparin's ability to sequester and sustain growth factor release, hepatocyte growth factor (HGF) was loaded into hydrogels made of either 7wt% type A GelNB or GelNB-Hep (R = 0.40 and R = 0.47, respectively). To account for the potential influence of heparin on gel crosslinking, the two gel formulations were tuned to yield almost identical stiffness (G' $\sim$5.5 kPa, Figure 4.11).

HGF-loaded type A GelNB or GelNB-Hep hydrogels were placed in PBS at 37°C and buffer aliquots were sampled at various time points for analyzing HGF release. As

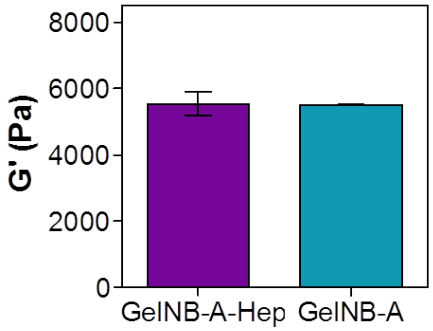

Fig. 4.11. Elastic modulus of 7 wt% type A GelNB and GelNB-Hep crosslinked by PEG4SH hydrogels used for HGF release.

shown in Figure 4.12, no significant difference in HGF release was observed between the two groups during the initial few hours of release. However, at 24 hours, significantly more HGF was released from the GelNB hydrogel than from GelNB-Hep gels. Nearly 400 hours into the release study, ∼17% of HGF was released from GelNB hydrogels and only about ∼7% of HGF was released from GelNB-Hep hydrogels. While the current study only demonstrates the ability of GelNB-Hep hydrogels to sequester and control the release of HGF, this gel format should have broader impact on supporting cell fate processes in 3D due to the broad affinity of heparin to various growth factors and cell-secreted proteins.

In order to ensure that the delay in release was in fact a result of heparin incorporation, negatively charged type B GelNB and GelNB-Hep was used. Previously others have found gelatin type B has a higher affinity for HGF over type A gelatin, and heparin possesses the highest affinity overall [49, 50]; however, with the incorporation of such a small amount of heparin, the environments may possess a similar degree of charge. Again hepatocyte growth factor (HGF) was loaded into hydrogels made of 7wt% GelNB-B-Hep or 7wt% GelNB-B (R = 0.45 and 0.50, respectively). Gel formulations resulted in hydrogels of similar stiffness (Figure 4.13) and therefore a similar crosslinking density in order to negate the impact of differences in network size on molecule diffusion within hydrogels.

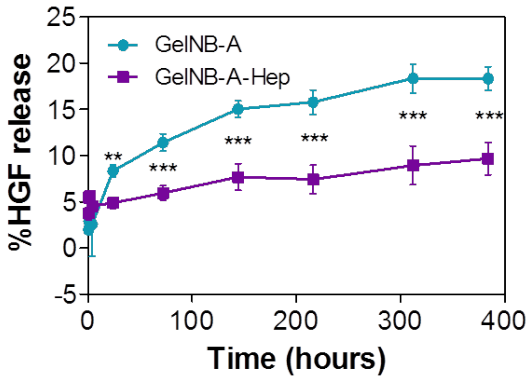

Fig. 4.12. Release of hepatocyte growth factor (HGF) from 7 wt% type A GelNB or GelNB-Hep gels crosslinked by PEG4SH (**p < 0.001; ***p < 0.0001).

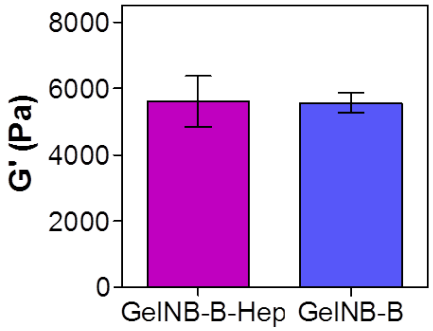

Fig. 4.13. Elastic modulus of 7 wt% type B GelNB and GelNB-Hep crosslinked by PEG4SH hydrogels used for HGF release.

Again, samples were collected at various time points and were analyzed to determine % HGF release. Figure 4.14 presents results obtained. As hypothesized, no significant differences can be observed between groups at any point in time. Typical release profiles can be seen during the first 80 hours, after which there is a sudden increase in release. This sudden increase may be a result of accelerated degradation of the hydrogel network. The lack of differences between release profiles is most likely due to the type of gelatin (type B) from which GelNB was originally synthesized.

Hydrogels contained 7 wt% GelNB-B-Hep indicating the incorporation of only 0.02 wt% heparin; therefore, as expected, an insufficient amount of heparin may have been conjugated onto the gelatin to achieve a difference in negative charge.

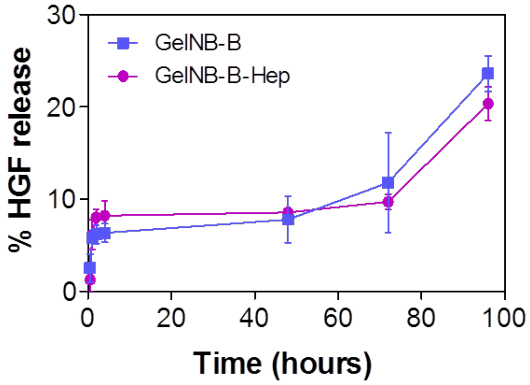

Fig. 4.14. Release of hepatocyte growth factor (HGF) from 7 wt% type B GelNB or GelNB-Hep gels crosslinked by PEG4SH

4.2 Investigate Hepatic Cell Viability and Functions in Modularly Crosslinked Gelatin Hydrogels

As mentioned earlier, liver cells must interact with their environment to receive or transmit signals for maintaining proper cell function. Huh7 cells were chosen here because of being a common cell type used for drug testing and for modeling liver cancer. We are interested in developing a tunable 3D biomimetic matrix to study liver cancer cell fate and this work is the first step towards establishing a therapeutically relevant biomimetic liver tumor niche. Utilizing the tunability of this particular thiol-ene system, this chapter focuses on the viability and functions of Huh7 cells as a result of being cultured within different formulations of GelNB hydrogels. Through percent survival, metabolic activity, CYP and urea functions, and confocal imaging, cell viability and functions were investigated.

4.2.1 Effect of Macromer Concentration on Gel Stability, Cell Viability, and Hepatocellular Functions

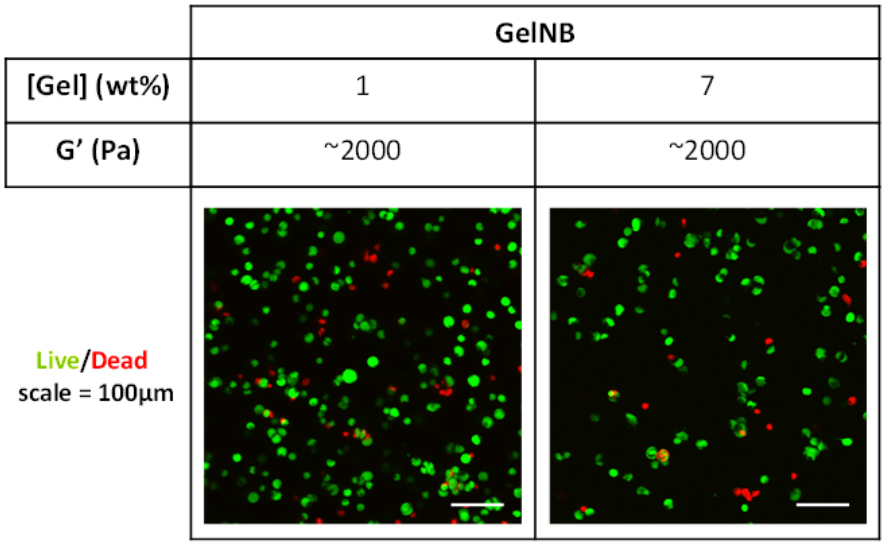

Fig. 4.15. Huh7 viability following encapsulation (day-0). Huh7 cells encapsulated in 1 wt% indicate viability levels similar to those encapsulated in 7 wt% of the same stiffness (∼85% and ∼87%, respectively).

To evaluate the effect of bioactive motif (i.e., gelatin content) on cell fate without the complication of different gel mechanical properties, we encapsulated Huh7 cells in modular GelNB hydrogels with increasing gelatin content (1-7 wt%) but with similar initial stiffness using formulations listed in Table 4.3. Live/Dead images were used for counting the percentage of live cells following light-mediated cell encapsulation (Figure 4.15, 1 and 7 wt% at ∼2000 Pa). With increasing gelatin concentration, the estimated viability of cells slightly increased from ∼85% to ∼87% for 1wt% and 7 wt%, respectively. Although all hydrogels include a similar concentration of cells ($5x10^6$ cells/mL), images obtained for 7 wt% GelNB gels present fewer cells compared with hydrogels comprised of 1 wt% GelNB of the same viewing area. With increasing gelatin content, it is expected that cells have a greater ability to degrade their envi-

ronment thereby leading to a larger degree of hydrogel swelling. This larger degree of swelling expands the environment of the cells resulting in a fewer cells per area.

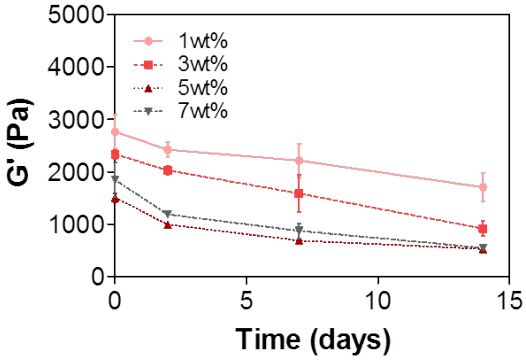

Fig. 4.16. Effect of Huh7 cells presence on gel properties. Shear moduli of cell-laden hydrogels over time.

Figure 4.16 further supports the differences in cell number shown in Figure 4.15. The presence of cells affected, although not statistically significantly, the initial moduli of the GelNB gels. Proteases secreted by Huh7 cells likely begin to degrade gelatin as soon as the cells were suspended in the pre-polymer solution. While the gel moduli in all gels decreased significantly over the course of 14 days, all hydrogels remained intact throughout the experiment indicating hydrogel stability.

To understand the effect of gelatin content on Huh7 viability, metabolic activity of the encapsulated cells was monitored over a two week period (Figure 4.17a). Huh7 cells encapsulated in gels with higher gelatin content (5 and 7 wt%) showed higher metabolic activity from day-2 to day-14 when compared to gels at lower gelatin content (e.g., 1 wt%). Cells encapsulated in 7 wt% GelNB showed significantly higher metabolic activity over all other groups by day-14 ($^*p < 0.05$).

When investigating the effect of macromer concentration on the viability of Huh7 cells, live/dead staining and confocal imaging results show that almost all cells remained alive and formed cell clusters in 5 and 7 wt% GelNB hydrogels whereas significantly more dead cells were found in hydrogels containing lower gelatin content

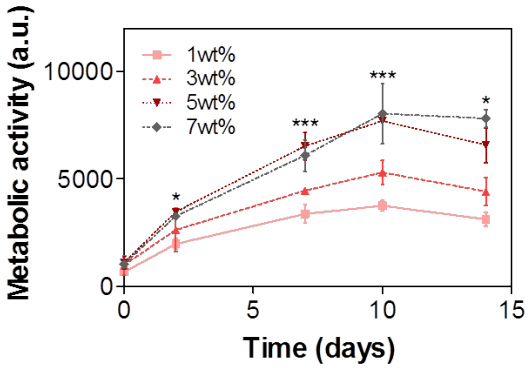

(a)

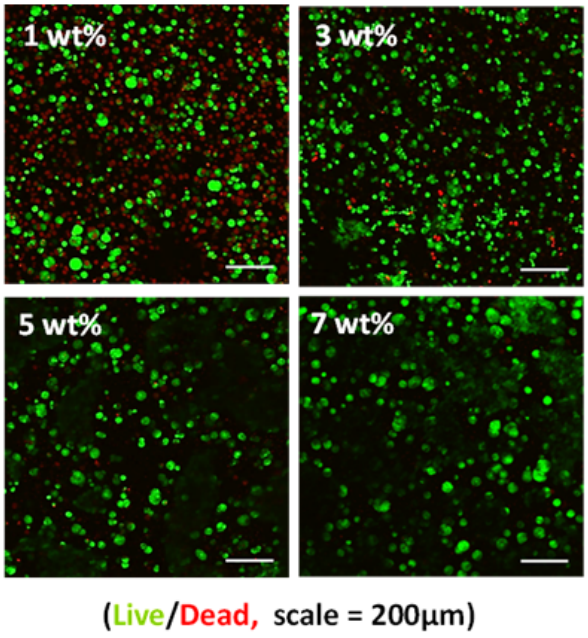

(b)

Fig. 4.17. Effect of type B GelNB content on Huh7 cell viability. (a) Metabolic activity of Huh7 cells as a function of time. (*$p < 0.05$, ***$p < 0.0001$). (b) Representative live/dead staining and confocal Z-stack images of encapsulated Huh7 cells on day 14.

(i.e., 1 and 3 wt% GelNB) (Figure 4.17b). These results demonstrate that higher gelatin or macromer content facilitates Huh7 cell survival.

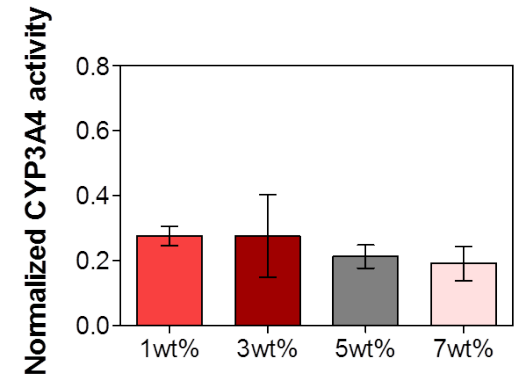

(a)

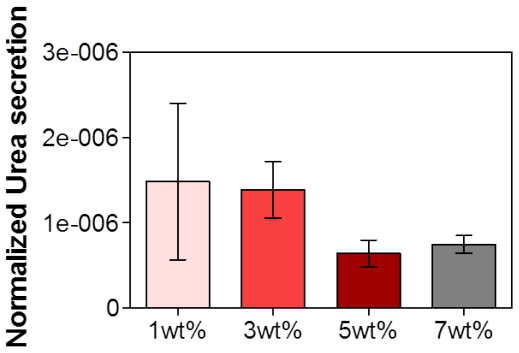

(b)

Fig. 4.18. Effect of type B GelNB content on Huh7 liver specific functions. (a) Normalized CYP3A4 enzymatic activity and (b) urea secretion from encapsulated Huh7 cells on day 14. CYP3A4 and urea levels were normalized to the metabolic activity on the same day of experiments.

One of the most important functions of the liver is the conversion of fat-soluble toxins into water-soluble waste, such as urea, by members of the CYP450 family. Among all the members of the CYP450 family, CYP34A is the most abundant enzyme. Therefore, CYP3A4 enzymatic activity (Figure 4.18a) and urea secretion (Figure 4.18b) were assessed to gain insight into the hepatocyte-specific function of the encapsulated cells. Interestingly, even though higher gelatin content improved cell survival (Figures 4.17a,b), CYP3A4 activity and urea secretion were not enhanced.

These results suggest that, in addition to the biological motifs provided by gelatin, additional ECM cues may be required to enhance cellular functions.

4.2.2 Effect of Thiol to Ene Ratio on Gel Stability, Cell Viability, and Hepatocellular Functions

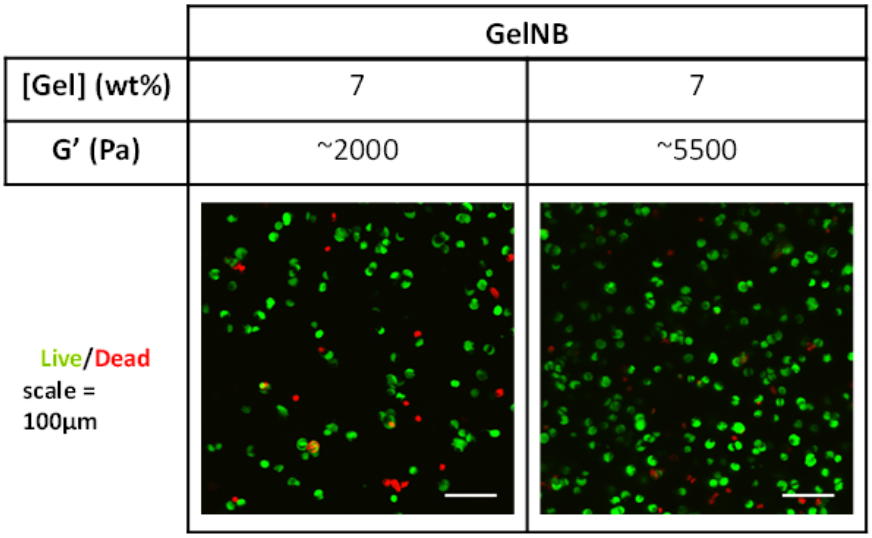

Fig. 4.19. Huh7 viability following encapsulation (day-0). Increasing the environment stiffness (or R-value) of encapsulated cells had little to no effect on viability compared to a softer environment (∼87% for 7 wt% 2000Pa (R = 0.34) and 5500 Pa (R = 0.75)).

Mechanical properties of 2D substrates or 3D matrices have been shown to affect cell fate processes. [51–53] While the mechanical properties of gelatin hydrogels formed by chain-growth polymerization can be tuned by adjusting functionalized gelatin content, this manipulation also simultaneously increases the concentrations of cell signaling motifs afforded by gelatin. We aimed to adjust the stiffness of our modularly crosslinked GelNB hydrogels for studying the effect of matrix mechanical cues on cell fate without the confounding effects of cell-ECM interactions. Since results shown in Figure 4.17 reveal that higher concentration of GelNB facilitates Huh7 cell

viability in 3D, we encapsulated Huh7 cells in gels containing 5 wt% GelNB while adjusting the R-value to yield the gels with a wide range of stiffness (G' ∼0.7 kPa to ∼5.5 kPa). Day-0 viability results obtained from single cells within 7 wt% indicate outcomes similar to that reported in the previous section; cell viability following encapsulation remained to be ∼87% as depicted in Figure 4.19.

Upon the encapsulation of Huh7 cells, all cell-laden GelNB hydrogels degraded over time but the moduli of the cell-laden hydrogels at day 14 were still significantly different from each other (Table 4.5 and Figure 4.20). The metabolic activity of Huh7 cells encapsulated in stiffer gels (R = 0.5 and 0.75) appeared to be suppressed when comparing with that in the softer gels (R = 0.34) (Figure 4.21a). A significant difference in metabolic activity was observed when cells were encapsulated in softer environments on day 7 and on-ward (***$p < 0.0001$). The results found here coincide with our previous findings that the metabolic activities of Huh7 cells were suppressed in stiffer hydrogels formed by PEG-based mixed-mode thiol-acrylate hydrogels. [54]

Table 4.5.
Hydrogel formulations used to tune moduli of hydrogels without affecting gelatin content.

	GelNB		**$PEG4SH_{10kDa}$**			**G' (Pa)**	
	wt%	**[ene](mM)**	**wt%**	**[thiol](mM)**	**R**	**Day0**	**Day14**
Q	5	11	0.9	3.7	0.34	1.50±0.09	0.52±0.06
R	5	11	1.4	5.6	0.50	3.76±0.30	2.42±0.10
S	5	11	2.1	8.4	0.75	6.90±0.12	5.40±0.40

Live/dead staining and confocal images indicate the effect of thiol to ene ratio (R) on cell viability (Figure 4.21b) as a result of being grown in GelNB hydrogels with different mechanical properties. Images captured on day-14 post-encapsulation demonstrated that cells were mostly alive and formed clusters with no distinct difference.

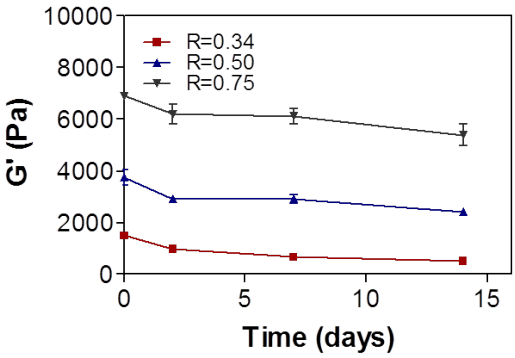

Fig. 4.20. Effect of Huh7 cells presence on gel properties. Stiffness of cell-laden hydrogels over time.

One would speculate that the decreased metabolic activity from cells encapsulated in stiffer gels was a result of cell death in stiffer gels. However, this was not the case for Huh7 cells encapsulated in GelNB hydrogels with different stiffness (Figure 4.21b). Huh7 cells encapsulated in stiffer GelNB hydrogels may have received increased mechanical stimuli that suppressed their cellular metabolic activity.

Matrix stiffness (G') at 3-6 kPa might be relevant in hepatocyte functions as this stiffness range is similar to the stiffness found in healthy liver ($<$ 6 kPa). [55] However, we found that CYP3A4 enzymatic activity was only slightly enhanced in cells grown in stiffer gels (R = 0.50 or 0.75. G' $\sim$5 kPa) at day 14 post-encapsulation (Figure 4.22a). The same trend was also found in urea secretion (Figure 4.22b). This result was different from our previous work where Huh7 cells encapsulated in bio-inert PEG-based thiol-acrylate hydrogels exhibited lower metabolic activity but higher urea secretion. [54] Future mechanistic studies are required to elucidate whether additional signaling crosstalks between integrins and mechanosensors exist in Huh7 cells that regulate protease activity and urea secretion.

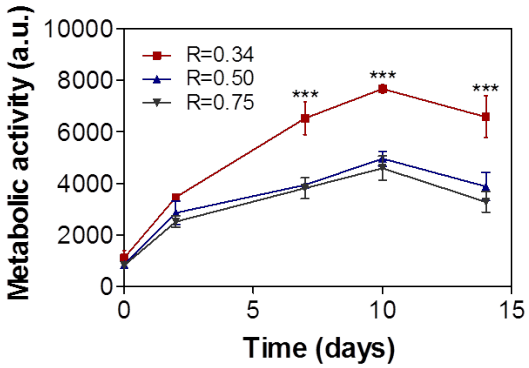

(a)

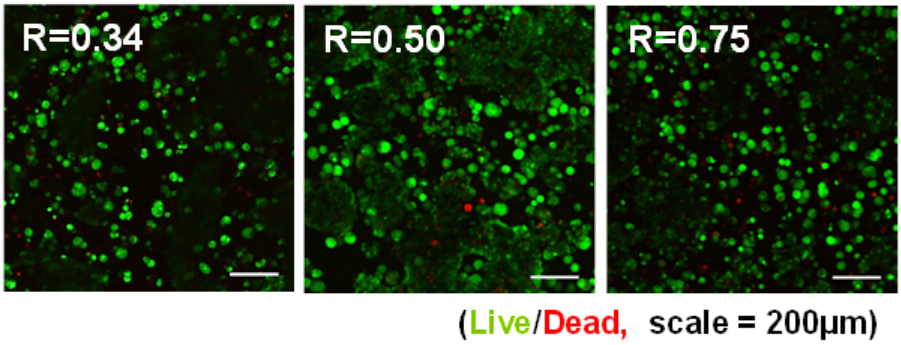

(b)

Fig. 4.21. Effect of matrix stiffness on Huh7 viability (formulations listed in Table 4.5). (a) Metabolic activity of encapsulated Huh7 cells as a function of time (***$p < 0.0001$). (b) Representative live/dead staining and confocal Z-stack images of encapsulated Huh7 cells in GelNB hydrogels on day 14.

4.3 Examine the Effect of Heparin Immobilization on Hepatic Cell Viability and Functions in 3D

Since adjusting the concentration of bioactive gelatin and matrix stiffness did not yield statistically significant differences in Huh7 cell functions, we sought to further modify GelNB hydrogels with other relevant bioactive motifs, such as heparin. After synthesis, the degree of heparin substitution on GelNB was about 0.003 wt% of heparin per 1 wt% of GelNB (or 3 μg heparin/mg GelNB). A previous study immobi-

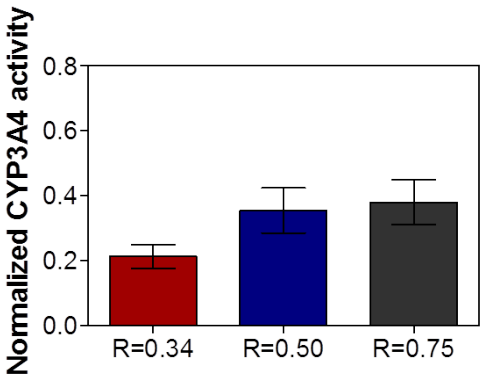

(a)

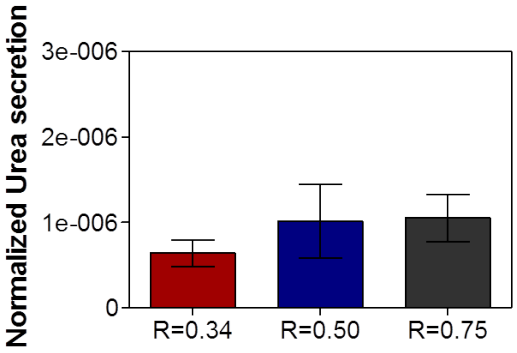

(b)

Fig. 4.22. Effect of matrix stiffness on Huh7 liver specific functions. (a) Normalized CYP3A4 enzymatic activity and (b) urea secretion from Huh7 cells cultured in gelatin based hydrogels on day 14. CYP3A4 and urea levels were normalized to the metabolic activity on the same day of experiments.

lized 1-7% (w/w) of heparin onto Gelatin/Tyramine and created vascular endothelial growth factor (VEGF) loaded hydrogels for the *in vitro* cell migration study of human umbilical vein endothelial cells (HUVECs) as well as an *in vivo* study of angiogenesis. In both experiments, protein bioactivity, cell migration, and angiogenesis were improved with the inclusion of heparin. [46] Compared to this system, our platform contains a much lower amount of heparin, therefore, the concentration used in our hydrogels must be favorable to cells.

4.3.1 Influence of Heparinization on Cell Viability and Hepatocellular Functions

Based on the viability results we saw with higher wt% GelNB hydrogels and the CYP3A4 function of cells within gels with increased stiffness, we sought to investigate the effect of heparin on Huh7 cells without the complications from gel stiffness and bioactive motifs. Here we prepared hydrogels with the same gelatin content (7 wt% type A GelNB and GelNB-Hep) and with similar stiffness (∼5.5 kPa). Following encapsulation of single cells on day-0, live dead images were obtained (Figure 4.23). Images indicate that the incorporation of heparin positively influenced the viability of cells immediately following polymerization resulting in fewer dead cells than can be seen in GelNB only gels. The viability of cells within GelNB hydrogels indicate ∼87% survival; whereas, cell survival within heparin conjugated GelNB hydrogels increases to greater than 95%.

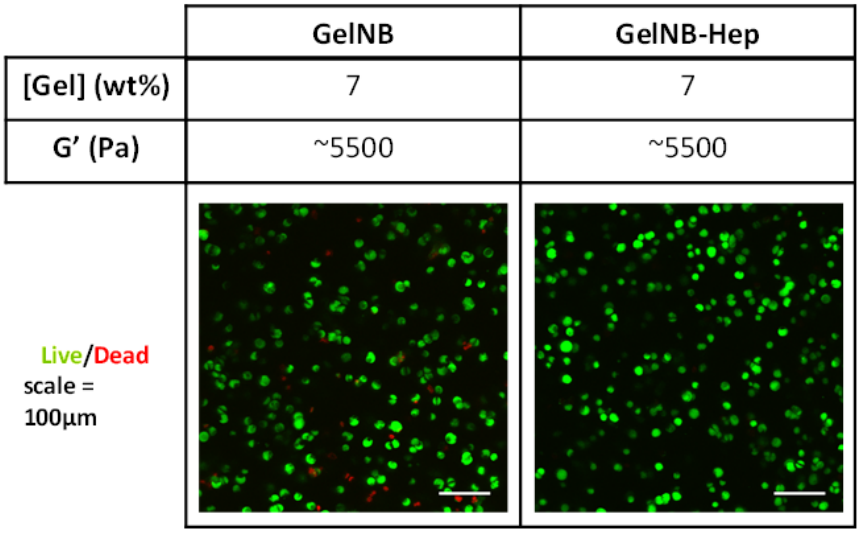

Fig. 4.23. Huh7 viability following encapsulation (day-0). The inclusion of heparin improved viability to greater than 95%.

Over time, huh7 cells encapsulated in GelNB and GelNB-Hep hydrogels remained viable, as demonstrated by the steady increase in metabolic activity (Figure 4.24a)

and live/dead staining (Figure 4.24b). However, Huh7 cells encapsulated in GelNB-Hep hydrogels showed significantly lower metabolic activity at days 7, 10, and 14 as compared with cells in GelNB hydrogels (**$p < 0.001$; ***$p < 0.0001$). Since the reduction of cell metabolic activity was not due to cell death (Figure 4.24b), it is logical to suggest that the immobilization of heparin altered intracellular signaling through sequestering growth factors contained in the supplemented serum (i.e., 10% FBS) or secreted by the encapsulated cells. It may be the case that cells are experiencing a state of quiescence while committing to a more defined phenotype; therefore, the inclusion of heparin possibly influenced a larger population of cells to enter this state of differentiation compared to those encapsulated in GelNB without heparin.

In addition to suppressing metabolic activity, immobilized heparin also significantly enhanced CYP450 enzymatic activity (Figure 4.25a) and urea secretion (Figure 4.25b). The enhanced hepatocyte-specific functions may be attributed to local enrichment of growth factors from serum through binding to immobilized heparin. Previously reported, FBS contains a number of growth factors, many of which have the ability to influence hepatocyte functions (i.e., TGFβ1, IGF-2, IGFBP2). [56, 57] TGFβ1 has been known to inhibit the growth of Huh7 cells and induce partial differentiation. [58] IGF-2 has been documented as a contributor in neoplastic hepatocyte proliferation (heterogeneous distribution of cells within a mass). [59] Therefore, the presence of heparin locally likely enriched some growth factors that synergistically enhance hepatocyte-specific functions. It is also possible that presence of heparin affected growth factor-receptor binding kinetics, which in turn resulted in different cell function.

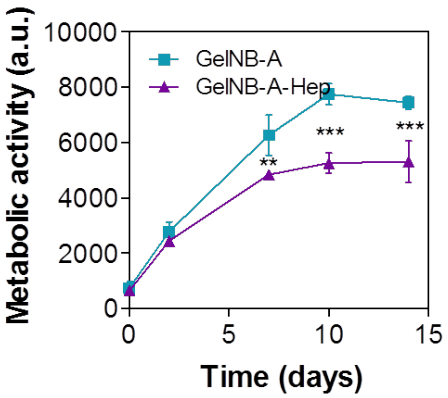

(a)

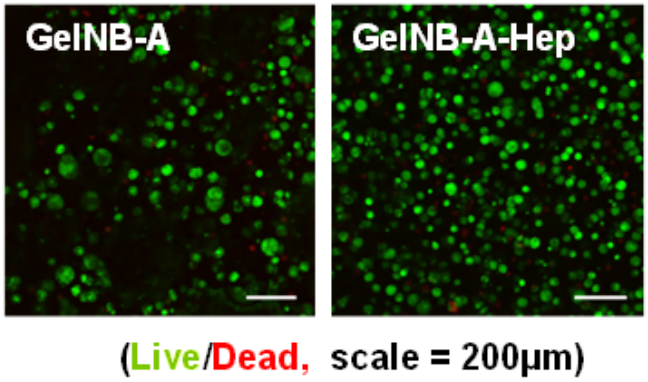

(b)

Fig. 4.24. Effect of heparin on Huh7 viability. (a) Effect of heparin on metabolic activity of Huh7 cells. (**p $<$ 0.001; ***p $<$ 0.0001). (b) Representative live/dead staining and confocal Z-stack images of encapsulated Huh7 cells in type A GelNB or GelNB-Hep hydrogels on day-14.

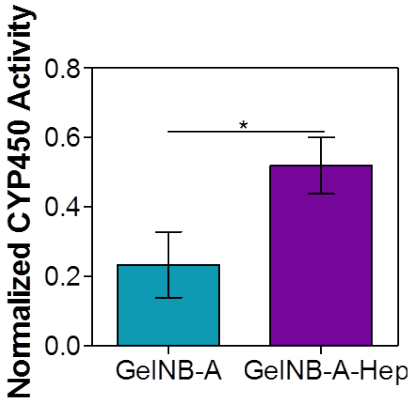

(a)

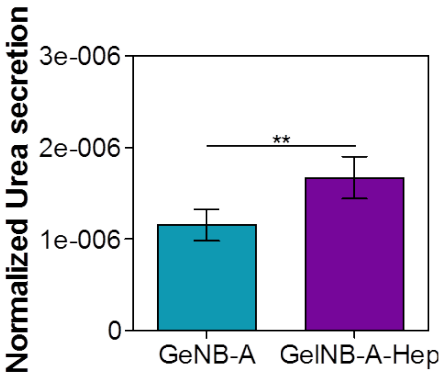

(b)

Fig. 4.25. Effect of heparin on hepatocellular functions. (a) Normalized CYP450 enzymatic activity in Huh7 cells cultured in gelatin based hydrogels on day-14 (*p $<$ 0.05). (b) Normalized urea secretion of Huh7 cells cultured in gelatin based hydrogels (**p $<$ 0.001).

5. SUMMARY

In summary, highly tunable gelatin-based hydrogels were prepared using orthogonal thiol-norbornene photochemistry. The biophysical and biochemical properties of GelNB hydrogels can be easily and independently tuned through adjusting the components in the precursor solution. As expected, these gelatin-based covalent hydrogels can be degraded by proteases. Although this natural platform can be degraded, gels remained stable for an extended period of time. The GelNB hydrogels are cytocompatible for *in vitro* 3D hepatocellular carcinoma cell culture. Through systemic variation of gelatin content and matrix stiffness, it was found that higher gelatin content and lower matrix stiffness promote cellular metabolic activity. However, suppressed metabolic activity does not necessarily correlate well with cell viability and function. The modularly crosslinked GelNB hydrogels were also modified with heparin to sequester growth factors and to positively influence CYP450 activity and urea secretion from encapsulated Huh7 cells. The ability to fine-tune matrix biophysical properties (e.g., stiffness) independent of biochemical properties (e.g., cell-responsive motifs) in gelatin hydrogels will allow researchers to study how independent local matrix properties affect cancer cell fate processes and drug responsiveness. Hence, the modularly crosslinked GelNB hydrogels should provide a highly favorable 3D cell culture platform for *in vitro* cancer cell research.

6. RECOMMENDATIONS

Future work will include the use of more relevant cell line to study the role of hepatic cells in liver regeneration and the differentiation of progenitor cells, such as HepaRG cells. HepaRG cells are classified as hepatoblasts and are immature epithelial cells with bipotent capabilities. These cells can be differentiated towards cholangiocytic (biliary) and hepatocytic cell lines. [3, 60] Unfortunately, differentiation requires the use of dimethyl sulfoxide (DMSO). DMSO is cytotoxic and its differentiation efficiency varies from batch to batch. [61] Based on the results obtained using Huh7 cells, it is hypothesized that this 3D culture system will provide the necessary environment to induce and maintain hepatocyte-specific functions required for HepaRG cell differentiation.

To investigate the differentiation of HepaRG cells, a controlled experiment was performed in 2D. Before exposure to DMSO, HepaRG cells appear to be of epithelial morphology as shown in phase contrast images (Fig. A.1 of the Appendix). After proliferating cells have reached confluency, 1% of DMSO is added to the media to induce cell differentiation. After one week of exposure to DMSO, cells begin to differentiate into cuboidal shaped hepatocytes or polygonal shaped cholangiocytes. 30 days of DMSO treatment result in the formation of hepatocyte clusters or islands and tightly packed polygonal cholangiocytes (Fig. A.2).

HepaRG cells were encapsulated in 7 wt% type A GelNB hydrogels with a stiffness of ∼2,000 Pa. After 7 days of culture within gels, half of the cell-laden hydrogels were subjected to DMSO treatment. Fig. A.3 presents live/dead images obtained on day 14 and metabolic activity of cells over the course of the experiment. Two distinct areas of growth can be seen in the live/dead images of each group. Prolif. 1 (Fig. A.3a) and Diff. 1 (Fig. A.3b) show that cells adapted a polygonal morphology that more closely resembles cholangiocytes. On the other hand, Prolif.2 and Diff. 2

show that cells adapted to a cuboidal morphology mimicking hepatocytes. Metabolic activity results indicate a dramatic decrease in activity upon the exposure of DMSO, a possible result of cell death (Fig. A.3c). This is further supported by the increased presence of dead cells seen in live/dead images. While additional studies are needed to verify these results, the preliminary work does indicate that our GelNB system has the potential to induce differentiation of HepaRG cells without using DMSO.

LIST OF REFERENCES

LIST OF REFERENCES

[1] T. T. Lau, L. Q. Lee, W. Leong, and D. A. Wang, "Formation of model hepatocellular aggregates in a hydrogel scaffold using degradable genipin crosslinked gelatin microspheres as cell carriers," *Biomed Mater*, vol. 7, no. 6, p. 065003, 2012. [Online]. Available: http://www.ncbi.nlm.nih.gov/pubmed/23117748

[2] P. Godoy, N. J. Hewitt, U. Albrecht, M. E. Andersen, N. Ansari, and S. Bhattacharya, "Recent advances in 2d and 3d in vitro systems using primary hepatocytes, alternative hepatocyte sources and non-parenchymal liver cells and their use in investigating mechanisms of hepatotoxicity, cell signaling and adme," *Arch Toxicol*, vol. 87, no. 8, pp. 1315–530, 2013. [Online]. Available: http://www.ncbi.nlm.nih.gov/pubmed/23974980

[3] M. M. Malinen, L. K. Kanninen, A. Corlu, H. M. Isoniemi, Y. R. Lou, M. L. Yliperttula, and A. O. Urtti, "Differentiation of liver progenitor cell line to functional organotypic cultures in 3d nanofibrillar cellulose and hyaluronan-gelatin hydrogels," *Biomaterials*, vol. 35, no. 19, pp. 5110–21, 2014. [Online]. Available: http://www.ncbi.nlm.nih.gov/pubmed/24698520

[4] T. Y. Lin, C. S. Ki, and C. C. Lin, "Manipulating hepatocellular carcinoma cell fate in orthogonally cross-linked hydrogels," *Biomaterials*, vol. 35, no. 25, pp. 6898–906, 2014. [Online]. Available: http://www.ncbi.nlm.nih.gov/pubmed/24857292

[5] D. L. Hoyert and J. Xu, "Deaths: preliminary data for 2011," *Natl Vital Stat Rep*, vol. 61, no. 6, pp. 1–51, 2012. [Online]. Available: http://www.ncbi.nlm.nih.gov/pubmed/24984457

[6] R. H. Wiesner, J. Rakela, M. B. Ishitani, D. C. Mulligan, J. R. Spivey, J. L. Steers, and R. A. Krom, "Recent advances in liver transplantation," *Mayo Clin Proc*, vol. 78, no. 2, pp. 197–210, 2003. [Online]. Available: http://www.ncbi.nlm.nih.gov/pubmed/12583530

[7] R. Hoekstra, G. A. Nibourg, T. V. van der Hoeven, G. Plomer, J. Seppen, M. T. Ackermans, S. Camus, W. Kulik, T. M. van Gulik, R. P. Elferink, and R. A. Chamuleau, "Phase 1 and phase 2 drug metabolism and bile acid production of heparg cells in a bioartificial liver in absence of dimethyl sulfoxide," *Drug Metab Dispos*, vol. 41, no. 3, pp. 562–7, 2013. [Online]. Available: http://www.ncbi.nlm.nih.gov/pubmed/23238784

[8] C. Guguen-Guillouzo and A. Guillouzo, "General review on in vitro hepatocyte models and their applications," *Methods Mol Biol*, vol. 640, pp. 1–40, 2010. [Online]. Available: http://www.ncbi.nlm.nih.gov/pubmed/20645044

[9] T. T. Lau, C. Wang, S. W. Png, K. Su, and D. A. Wang, "Genipin-crosslinked microcarriers mediating hepatocellular aggregates formation and functionalities," *J Biomed Mater Res A*, vol. 96, no. 1, pp. 204–11, 2011. [Online]. Available: http://www.ncbi.nlm.nih.gov/pubmed/21105169

[10] R. C. Dutta and A. K. Dutta, "Cell-interactive 3d-scaffold; advances and applications," *Biotechnol Adv*, vol. 27, no. 4, pp. 334–9, 2009. [Online]. Available: http://www.ncbi.nlm.nih.gov/pubmed/19232387

[11] J. Rose, S. Pacelli, A. Haj, H. Dua, A. Hopkinson, L. White, and F. Rose, "Gelatin-based materials in ocular tissue engineering," *Materials*, vol. 7, no. 4, pp. 3106–3135, 2014. [Online]. Available: http://www.mdpi.com/1996-1944/7/4/3106

[12] S. Singh, K. Rao, K. Venugopal, and R. Manikandan, "Alteration in dissolution characteristics of gelatin-containing formulations: A review of the problem, test methods, and solutions."," *Pharmaceutical Technology.*, 2002.

[13] Z. Munoz, H. Shih, and C.-C. Lin, "Gelatin hydrogels formed by orthogonal thiol-norbornene photochemistry for cell encapsulation," *Biomaterials Science*, vol. 2, no. 8, pp. 1063–1072, 2014. [Online]. Available: http://dx.doi.org/10.1039/C4BM00070F

[14] E. Kaemmerer, F. P. Melchels, B. M. Holzapfel, T. Meckel, D. W. Hutmacher, and D. Loessner, "Gelatine methacrylamide-based hydrogels: an alternative three-dimensional cancer cell culture system," *Acta Biomater*, vol. 10, no. 6, pp. 2551–62, 2014. [Online]. Available: http://www.ncbi.nlm.nih.gov/pubmed/24590158

[15] G. Camci-Unal, D. Cuttica, N. Annabi, D. Demarchi, and A. Khademhosseini, "Synthesis and characterization of hybrid hyaluronic acid-gelatin hydrogels," *Biomacromolecules*, vol. 14, no. 4, pp. 1085–92, 2013. [Online]. Available: http://www.ncbi.nlm.nih.gov/pubmed/23419055

[16] H. B. Renani, M. Ghorbani, B. H. Beni, Z. Karimi, M. Mirhosseini, H. Zarkesh, and A. Kabiri, "Determination and comparison of specifics of nucleus pulposus cells of human intervertebral disc in alginate and chitosan-gelatin scaffolds," *Adv Biomed Res*, vol. 1, p. 81, 2012. [Online]. Available: http://www.ncbi.nlm.nih.gov/pubmed/23326811

[17] F. L. Mi, Y. C. Tan, H. C. Liang, R. N. Huang, and H. W. Sung, "In vitro evaluation of a chitosan membrane cross-linked with genipin," *J Biomater Sci Polym Ed*, vol. 12, no. 8, pp. 835–50, 2001. [Online]. Available: http://www.ncbi.nlm.nih.gov/pubmed/11718480

[18] K. Yue, G. Trujillo-de Santiago, M. M. Alvarez, A. Tamayol, N. Annabi, and A. Khademhosseini, "Synthesis, properties, and biomedical applications of gelatin methacryloyl (gelma) hydrogels," *Biomaterials*, vol. 73, pp. 254–271, 2015. [Online]. Available: http://www.ncbi.nlm.nih.gov/pubmed/26414409

[19] A. I. Van Den Bulcke, B. Bogdanov, N. De Rooze, E. H. Schacht, M. Cornelissen, and H. Berghmans, "Structural and rheological properties of methacrylamide modified gelatin hydrogels," *Biomacromolecules*, vol. 1, no. 1, pp. 31–8, 2000. [Online]. Available: http://www.ncbi.nlm.nih.gov/pubmed/11709840

[20] Y. Zuo, X. Liu, D. Wei, J. Sun, W. Xiao, H. Zhao, L. Guo, Q. Wei, H. Fan, and X. Zhang, "Photo-cross-linkable methacrylated gelatin and hydroxyapatite hybrid hydrogel for modularly engineering biomimetic osteon," *ACS Appl Mater Interfaces*, vol. 7, no. 19, pp. 10 386–94, 2015. [Online]. Available: http://www.ncbi.nlm.nih.gov/pubmed/25928732

[21] X. Zhao, Q. Lang, L. Yildirimer, Z. Y. Lin, W. Cui, N. Annabi, K. W. Ng, M. R. Dokmeci, A. M. Ghaemmaghami, and A. Khademhosseini, "Photocrosslinkable gelatin hydrogel for epidermal tissue engineering," *Adv Healthc Mater*, 2015. [Online]. Available: http://www.ncbi.nlm.nih.gov/pubmed/25880725

[22] J. Visser, P. A. Levett, N. C. te Moller, J. Besems, K. W. Boere, M. H. van Rijen, J. C. de Grauw, W. J. Dhert, P. R. van Weeren, and J. Malda, "Crosslinkable hydrogels derived from cartilage, meniscus, and tendon tissue," *Tissue Eng Part A*, vol. 21, no. 7-8, pp. 1195–206, 2015. [Online]. Available: http://www.ncbi.nlm.nih.gov/pubmed/25557049

[23] E. Gevaert, T. Billiet, H. Declercq, P. Dubruel, and R. Cornelissen, "Galactose-functionalized gelatin hydrogels improve the functionality of encapsulated hepg2 cells," *Macromol Biosci*, vol. 14, no. 3, pp. 419–27, 2014. [Online]. Available: http://www.ncbi.nlm.nih.gov/pubmed/24821670

[24] J. Visser, D. Gawlitta, K. E. Benders, S. M. Toma, B. Pouran, P. R. van Weeren, W. J. Dhert, and J. Malda, "Endochondral bone formation in gelatin methacrylamide hydrogel with embedded cartilage-derived matrix particles," *Biomaterials*, vol. 37, pp. 174–82, 2015. [Online]. Available: http://www.ncbi.nlm.nih.gov/pubmed/25453948

[25] P. Kim, A. Yuan, K. H. Nam, A. Jiao, and D. H. Kim, "Fabrication of poly(ethylene glycol): gelatin methacrylate composite nanostructures with tunable stiffness and degradation for vascular tissue engineering," *Biofabrication*, vol. 6, no. 2, p. 024112, 2014. [Online]. Available: http://www.ncbi.nlm.nih.gov/pubmed/24717683

[26] H. Wang, L. Zhou, J. Liao, Y. Tan, K. Ouyang, C. Ning, G. Ni, and G. Tan, "Cell-laden photocrosslinked gelma-dexma copolymer hydrogels with tunable mechanical properties for tissue engineering," *J Mater Sci Mater Med*, vol. 25, no. 9, pp. 2173–83, 2014. [Online]. Available: http://www.ncbi.nlm.nih.gov/pubmed/25008369

[27] J. A. Benton, C. A. DeForest, V. Vivekanandan, and K. S. Anseth, "Photocrosslinking of gelatin macromers to synthesize porous hydrogels that promote valvular interstitial cell function," *Tissue Eng Part A*, vol. 15, no. 11, pp. 3221–30, 2009. [Online]. Available: http://www.ncbi.nlm.nih.gov/pubmed/19374488

[28] J. W. Nichol, S. T. Koshy, H. Bae, C. M. Hwang, S. Yamanlar, and A. Khademhosseini, "Cell-laden microengineered gelatin methacrylate hydrogels," *Biomaterials*, vol. 31, no. 21, pp. 5536–44, 2010. [Online]. Available: http://www.ncbi.nlm.nih.gov/pubmed/20417964

[29] H. Bae, A. F. Ahari, H. Shin, J. W. Nichol, C. B. Hutson, M. Masaeli, S. H. Kim, H. Aubin, S. Yamanlar, and A. Khademhosseini, "Cell-laden microengineered pullulan methacrylate hydrogels promote cell proliferation and 3d cluster formation," *Soft Matter*, vol. 7, no. 5, pp. 1903–1911, 2011. [Online]. Available: http://www.ncbi.nlm.nih.gov/pubmed/21415929

[30] B. D. Fairbanks, M. P. Schwartz, A. E. Halevi, C. R. Nuttelman, C. N. Bowman, and K. S. Anseth, "A versatile synthetic extracellular matrix mimic via thiol-norbornene photopolymerization," *Adv Mater*, vol. 21, no. 48, pp. 5005–10, 2009. [Online]. Available: http://www.ncbi.nlm.nih.gov/pubmed/25377720

[31] C. C. Lin, A. Raza, and H. Shih, "Peg hydrogels formed by thiol-ene photo-click chemistry and their effect on the formation and recovery of insulin-secreting cell spheroids," *Biomaterials*, vol. 32, no. 36, pp. 9685–95, 2011. [Online]. Available: http://www.ncbi.nlm.nih.gov/pubmed/21924490

[32] J. D. McCall and K. S. Anseth, "Thiol-ene photopolymerizations provide a facile method to encapsulate proteins and maintain their bioactivity," *Biomacromolecules*, vol. 13, no. 8, pp. 2410–7, 2012. [Online]. Available: http://www.ncbi.nlm.nih.gov/pubmed/22741550

[33] B. V. Sridhar, J. L. Brock, J. S. Silver, J. L. Leight, M. A. Randolph, and K. S. Anseth, "Development of a cellularly degradable peg hydrogel to promote articular cartilage extracellular matrix deposition," *Adv Healthc Mater*, vol. 4, no. 5, pp. 702–13, 2015. [Online]. Available: http://www.ncbi.nlm.nih.gov/pubmed/25607633

[34] H. Shih and C. C. Lin, "Cross-linking and degradation of step-growth hydrogels formed by thiol-ene photoclick chemistry," *Biomacromolecules*, vol. 13, no. 7, pp. 2003–12, 2012. [Online]. Available: http://www.ncbi.nlm.nih.gov/pubmed/22708824

[35] A. Raza and C. C. Lin, "The influence of matrix degradation and functionality on cell survival and morphogenesis in peg-based hydrogels," *Macromol Biosci*, vol. 13, no. 8, pp. 1048–58, 2013. [Online]. Available: http://www.ncbi.nlm.nih.gov/pubmed/23776086

[36] C. B. Hutson, J. W. Nichol, H. Aubin, H. Bae, S. Yamanlar, S. Al-Haque, S. T. Koshy, and A. Khademhosseini, "Synthesis and characterization of tunable poly(ethylene glycol): gelatin methacrylate composite hydrogels," *Tissue Eng Part A*, vol. 17, no. 13-14, pp. 1713–23, 2011. [Online]. Available: http://www.ncbi.nlm.nih.gov/pubmed/21306293

[37] M. Kim, J. Y. Lee, C. N. Jones, A. Revzin, and G. Tae, "Heparin-based hydrogel as a matrix for encapsulation and cultivation of primary hepatocytes," *Biomaterials*, vol. 31, no. 13, pp. 3596–603, 2010. [Online]. Available: http://www.ncbi.nlm.nih.gov/pubmed/20153045

[38] S. Nakamura, T. Kubo, and H. Ijima, "Heparin-conjugated gelatin as a growth factor immobilization scaffold," *J Biosci Bioeng*, vol. 115, no. 5, pp. 562–7, 2013. [Online]. Available: http://www.ncbi.nlm.nih.gov/pubmed/23273911

[39] J. Lee, J. J. Yoo, A. Atala, and S. J. Lee, "The effect of controlled release of pdgf-bb from heparin-conjugated electrospun pcl/gelatin scaffolds on cellular bioactivity and infiltration," *Biomaterials*, vol. 33, no. 28, pp. 6709–20, 2012. [Online]. Available: http://www.ncbi.nlm.nih.gov/pubmed/22770570

[40] J. You, D. S. Shin, D. Patel, Y. Gao, and A. Revzin, "Multilayered heparin hydrogel microwells for cultivation of primary hepatocytes," *Adv Healthc Mater*, vol. 3, no. 1, pp. 126–32, 2014. [Online]. Available: http://www.ncbi.nlm.nih.gov/pubmed/23828859

[41] S. Kato, T. Ishii, H. Hara, N. Sugiura, K. Kimata, and N. Akamatsu, "Hepatocyte growth factor immobilized onto culture substrates through heparin and matrigel enhances dna synthesis in primary rat hepatocytes," *Exp Cell Res*, vol. 211, no. 1, pp. 53–8, 1994. [Online]. Available: http://www.ncbi.nlm.nih.gov/pubmed/8125158

[42] H. Francis and C. J. Meininger, "A review of mast cells and liver disease: What have we learned?" *Dig Liver Dis*, vol. 42, no. 8, pp. 529–36, 2010. [Online]. Available: http://www.ncbi.nlm.nih.gov/pubmed/20363674

[43] M. Lyon, J. A. Deakin, H. Rahmoune, D. G. Fernig, T. Nakamura, and J. T. Gallagher, "Hepatocyte growth factor/scatter factor binds with high affinity to dermatan sulfate," *J Biol Chem*, vol. 273, no. 1, pp. 271–8, 1998. [Online]. Available: http://www.ncbi.nlm.nih.gov/pubmed/9417075

[44] H. Ijima, T. Matsuo, and K. Kawakami, "The mixed coculture effect of primary rat hepatocytes and bone marrow cells is caused by soluble factors derived from bone marrow cells," *J Biosci Bioeng*, vol. 105, no. 3, pp. 226–31, 2008. [Online]. Available: http://www.ncbi.nlm.nih.gov/pubmed/18397773

[45] Y. T. Hou, H. Ijima, S. Matsumoto, T. Kubo, T. Takei, S. Sakai, and K. Kawakami, "Effect of a hepatocyte growth factor/heparin-immobilized collagen system on albumin synthesis and spheroid formation by hepatocytes," *J Biosci Bioeng*, vol. 110, no. 2, pp. 208–16, 2010. [Online]. Available: http://www.ncbi.nlm.nih.gov/pubmed/20547342

[46] Z. Li, T. Qu, C. Ding, C. Ma, H. Sun, S. Li, and X. Liu, "Injectable gelatin derivative hydrogels with sustained vascular endothelial growth factor release for induced angiogenesis," *Acta Biomater*, vol. 13, pp. 88–100, 2015. [Online]. Available: http://www.ncbi.nlm.nih.gov/pubmed/25462840

[47] G. Niu, J. S. Choi, Z. Wang, A. Skardal, M. Giegengack, and S. Soker, "Heparin-modified gelatin scaffolds for human corneal endothelial cell transplantation," *Biomaterials*, vol. 35, no. 13, pp. 4005–14, 2014. [Online]. Available: http://www.ncbi.nlm.nih.gov/pubmed/24508079

[48] L. Hedstrom, L. Szilagyi, and W. J. Rutter, "Converting trypsin to chymotrypsin: the role of surface loops," *Science*, vol. 255, no. 5049, pp. 1249–53, 1992. [Online]. Available: http://www.ncbi.nlm.nih.gov/pubmed/1546324

[49] M. Ozeki and Y. Tabata, "Interaction of hepatocyte growth factor with gelatin as the carrier material," *J Biomater Sci Polym Ed*, vol. 17, no. 1-2, pp. 163–75, 2006. [Online]. Available: http://www.ncbi.nlm.nih.gov/pubmed/16411606

[50] M. Ozeki, "Affinity evaluation of gelatin for hepatocyte growth factor of different types to design the release carrier," *J Biomater Sci Polym Ed*, vol. 17, no. 1-2, pp. 139–50, 2006. [Online]. Available: http://www.ncbi.nlm.nih.gov/pubmed/16411604

[51] A. B. Pratt, F. E. Weber, H. G. Schmoekel, R. Muller, and J. A. Hubbell, "Synthetic extracellular matrices for in situ tissue engineering," *Biotechnol Bioeng*, vol. 86, no. 1, pp. 27–36, 2004. [Online]. Available: http://www.ncbi.nlm.nih.gov/pubmed/15007838

[52] S. R. Peyton, C. M. Ghajar, C. B. Khatiwala, and A. J. Putnam, "The emergence of ecm mechanics and cytoskeletal tension as important regulators of cell function," *Cell Biochem Biophys*, vol. 47, no. 2, pp. 300–20, 2007. [Online]. Available: http://www.ncbi.nlm.nih.gov/pubmed/17652777

[53] A. M. Kloxin, C. J. Kloxin, C. N. Bowman, and K. S. Anseth, "Mechanical properties of cellularly responsive hydrogels and their experimental determination," *Adv Mater*, vol. 22, no. 31, pp. 3484–94, 2010. [Online]. Available: http://www.ncbi.nlm.nih.gov/pubmed/20473984

[54] Y. Hao and C. C. Lin, "Degradable thiol-acrylate hydrogels as tunable matrices for three-dimensional hepatic culture," *J Biomed Mater Res A*, vol. 102, no. 11, pp. 3813–27, 2014. [Online]. Available: http://www.ncbi.nlm.nih.gov/pubmed/24288169

[55] J. You, S. A. Park, D. S. Shin, D. Patel, V. K. Raghunathan, M. Kim, C. J. Murphy, G. Tae, and A. Revzin, "Characterizing the effects of heparin gel stiffness on function of primary hepatocytes," *Tissue Eng Part A*, vol. 19, no. 23-24, pp. 2655–63, 2013. [Online]. Available: http://www.ncbi.nlm.nih.gov/pubmed/23815179

[56] X. Zheng, H. Baker, W. S. Hancock, F. Fawaz, M. McCaman, and J. Pungor, E., "Proteomic analysis for the assessment of different lots of fetal bovine serum as a raw material for cell culture. part iv. application of proteomics to the manufacture of biological drugs," *Biotechnol Prog*, vol. 22, no. 5, pp. 1294–300, 2006. [Online]. Available: http://www.ncbi.nlm.nih.gov/pubmed/17022666

[57] T. Oida and H. L. Weiner, "Depletion of tgf-beta from fetal bovine serum," *J Immunol Methods*, vol. 362, no. 1-2, pp. 195–8, 2010. [Online]. Available: http://www.ncbi.nlm.nih.gov/pubmed/20837018

[58] B. Damdinsuren, H. Nagano, M. Kondo, J. Natsag, H. Hanada, M. Nakamura, H. Wada, H. Kato, S. Marubashi, A. Miyamoto, Y. Takeda, K. Umeshita, K. Dono, and M. Monden, "Tgf-beta1-induced cell growth arrest and partial differentiation is related to the suppression of id1 in human hepatoma cells," *Oncol Rep*, vol. 15, no. 2, pp. 401–8, 2006. [Online]. Available: http://www.ncbi.nlm.nih.gov/pubmed/16391861

[59] C. Morace, M. Cucunato, R. Bellerone, G. De Caro, S. Crino, A. Fortiguerra, F. Spadaro, A. Zirilli, A. Alibrandi, P. Consolo, C. Luigiano, M. L. Resta, O. Ferrau, and A. Spadaro, "Insulin-like growth factor-ii is a useful marker to detect hepatocellular carcinoma?" *Eur J Intern Med*, vol. 23, no. 6, pp. e157–61, 2012. [Online]. Available: http://www.ncbi.nlm.nih.gov/pubmed/22863442

[60] V. Cerec, D. Glaise, D. Garnier, S. Morosan, B. Turlin, B. Drenou, P. Gripon, D. Kremsdorf, C. Guguen-Guillouzo, and A. Corlu, "Transdifferentiation of hepatocyte-like cells from the human hepatoma heparg cell line through bipotent progenitor," *Hepatology*, vol. 45, no. 4, pp. 957–67, 2007. [Online]. Available: http://www.ncbi.nlm.nih.gov/pubmed/17393521

[61] S. P. Rebelo, R. Costa, M. Estrada, V. Shevchenko, C. Brito, and P. M. Alves, "Heparg microencapsulated spheroids in dmso-free culture: novel culturing approaches for enhanced xenobiotic and biosynthetic metabolism," *Arch Toxicol*, vol. 89, no. 8, pp. 1347–58, 2015. [Online]. Available: http://www.ncbi.nlm.nih.gov/pubmed/25107451

APPENDIX

APPENDIX: HepaRG DATA

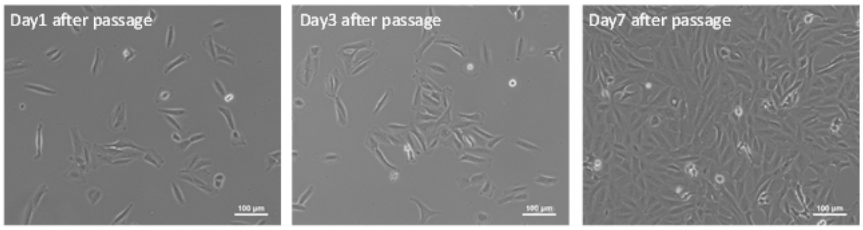

Fig. A.1. Undifferentiated HepaRG cells plated at 1.6 million/plate (standard TCP) for proliferation. Cells appear clear and epithelial-like.

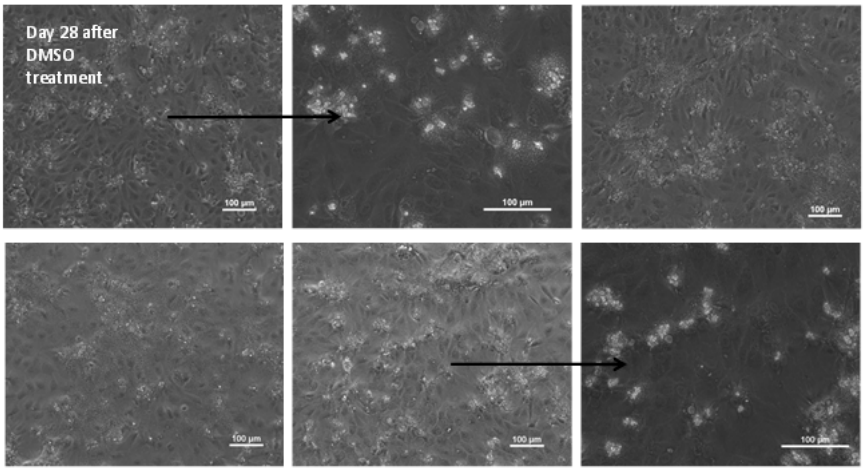

Fig. A.2. Plated 0.8 million cells/well (6-wellplate) for differentiation and allowed cells to reach 90% confluency. Then cells were subjected to 1% DMSO. Nearly 30 days of DMSO exposure lead to the formation of hepatocyte isles, a result of the differentiation of HepaRG cells.

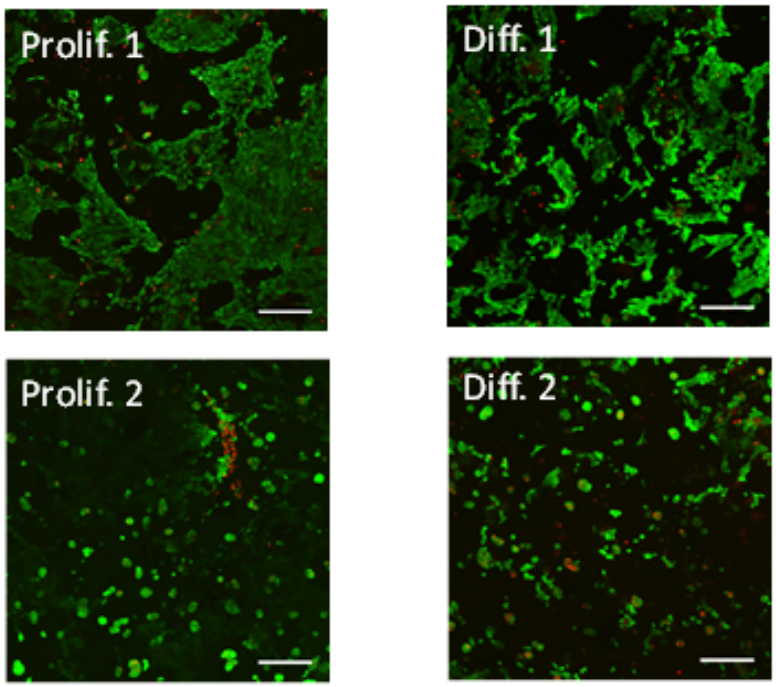

(a) (b)

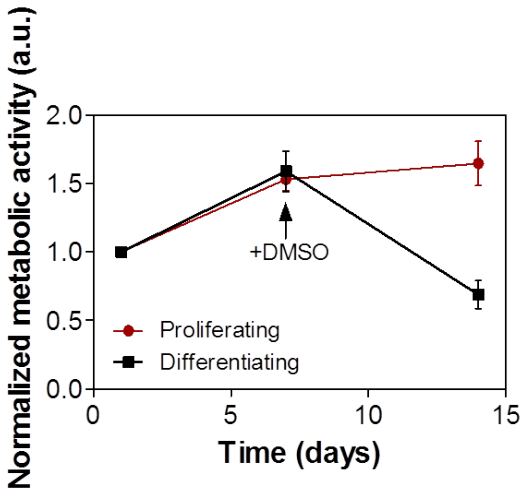

(c)

Fig. A.3. (a) Representative live/dead staining and confocal Z-stack images of encapsulated proliferating HepaRG cells in type A GelNB hydrogels on day 14 without DMSO exposure and (b) with DMSO exposure. (c) Effect of DMSO exposure on metabolic activity of HepaRG cells.